Elsevier Editorial System(tm) for Journal of Applied Geophysics
Manuscript Draft

Manuscript Number: APPGEO2138R2

Title: The electrical properties of calcium sulphate rocks from decametric to micrometic scale

Article Type: Review Article

Keywords: Gypsum, Anhydrite, Sulphate, Electrical Conductivity

Corresponding Author: Dr Ander Guinea,

Corresponding Author's Institution: University of Barcelona

First Author: Ander Guinea

Order of Authors: Ander Guinea; Elisabet Playà; Lluís Rivero; Juan José Ledo; Pilar Queralt

Abstract: Sulphate rocks have a sedimentary evaporitic origin and are present in many deposits worldwide. Among them, gypsum (dihydrated calcium sulphate) is the most common and is exploited for industrial purposes. Anhydrite (calcium sulphate) is frequently found in gypsum quarries and in non-outcropping sulphates. The greater hardness of anhydrite compared to gypsum causes a problem for gypsum extraction; quarry fronts have to be halted as soon as anhydrite is found. In this work the electrical properties of calcium sulphates have been studied by means of geoelectrical methods.

A direct relationship between the electrical conductivity values of the calcium sulphate rocks and their lithological composition has been established with the lutitic matrix being the main controlling factor when it is well connected. When the matrix is under the percolation threshold the sulphate phases are dominant, and the electrical response of the rocks depends on the percentage of each phase. When the rock is matrix dominant, the electrical resistivity trend fits with the Hashin-Shtrikman lower bound for multiphase systems (considering gypsum, anhydrite and matrix as the components). On the other hand, when the rock is calcium sulphate dominant the trend shows the one of the Hashin-Shtrikman upper bound. The reference electrical resistivity value of pure anhydrite rocks has been defined as 104 Ω.m and geoelectrical classification for calcium sulphate rocks has been elaborated. With this classification it is possible to differentiate between calcium sulphate rocks with different composition from their electrical resistivity value. This classification has been checked with field examples and calculating the theoretical resistivity value of thin section photographs with the program ELECFEM2D. The electrical behavior of calcium sulphate rocks is a good reference for other type of rocks with electrically differentiated components, and similar methods can be used to define their geoelectrical responses.

A direct relationship between the electrical conductivity values of the calcium sulphate rocks and their lithological composition has been established being the lutitic matrix the main controlling factor when it is percolant (connected at long range). When the matrix is under the percolation threshold the dominant phases are the sulphate ones and the electrical response of the rocks depends on the percentage of each one in their composition. When the rock is matrix dominant, the electrical resistivity trend fits with the Hashin-Shtrikman lower bound for multiphase systems (considering gypsum, anhydrite and matrix as the components). On the other hand, when the rock is calcium sulphate dominant the trend shows the one of the Hashin-Shtrikman upper bound. The reference

electrical resistivity value of pure anhydrite rocks has been defined as 104 ohm.m and geoelectrical classification for calcium sulphate rocks has been elaborated. With this classification it is possible to differentiate between calcium sulphate rocks with different composition from their electrical resistivity value. This classification has been checked with field examples and calculating the theoretical resistivity value of thin section photographs with the program ELECFEM2D. The electrical behavior of calcium sulphate rocks is a good reference for other type of rocks with electrically differentiated components, and similar methods can be used to define their geoelectrical responses.

Research Highlights

In this paper the electrical conductivity of Sulphate Rocks is studied. > Electrical Resistivity Tomography profiles are performed. > Conductivity measures are carried out in laboratory conditions. > The conductivity of sulphate rocks is theoretically calculated at microscopic scale from microphotographs. > An electrical classification of sulphate rocks has been elaborated.

Revision Notes 2nd review

Click here to download Revision Notes: Revision notes 2nd review.docx

Dear editor and reviewers,

I have performed the changes in the model calculated with the modified Archie's law using the coefficients suggested. I also have made some little changes in the text (marked in red) and in some figures (figures 4 and 6 and table 4) as required by the reviewer Paul Glover. I want to thank him for his comments because I really think that the quality of the paper has increased since the first submission thanks to them.

Yours sincerely

Ander Guinea and co-authors

University of Barcelona

THE ELECTRICAL PROPERTIES OF CALCIUM SULPHATE ROCKS FROM DECAMETRIC TO MICROMETRIC SCALE

Ander Guinea[1]*, Elisabet Playà[1], Lluís Rivero[1], Juan José Ledo[2], Pilar Queralt[2]

[1]*Departament de Geoquímica, Petrologia i Prospecció Geològica. Facultat de Geologia, Universitat de Barcelona (UB). Martí i Franquès s/n, 08028 Barcelona, Spain.*

[2]*Departament de Geodinàmica i Geofísica. Facultat de Geologia, Universitat de Barcelona (UB). Martí i Franquès s/n, 08028 Barcelona, Spain.*

E-mails: anderguinea@ub.edu; eplaya@ub.edu; lrivero@ub.edu; jledo@ub.edu; pilar.queralt@ub.edu

*Corresponding author: *Phone number: +34 934 03 11 65. Fax number: +34 934 02 14 17*

ABSTRACT

Sulphate rocks have a sedimentary evaporitic origin and are present in many deposits worldwide. Among them, gypsum (dihydrated calcium sulphate) is the most common and is exploited for industrial purposes. Anhydrite (calcium sulphate) is frequently found in gypsum quarries and in non-outcropping sulphates. The greater hardness of anhydrite compared to gypsum causes a problem for gypsum extraction; quarry fronts have to be halted as soon as anhydrite is found. In this work the electrical properties of calcium sulphates have been studied by means of geoelectrical methods.

A direct relationship between the electrical conductivity values of the calcium sulphate rocks and their lithological composition has been established with the lutitic matrix being the main controlling factor when it is well connected. When the matrix is under the percolation threshold the sulphate phases are dominant, and the electrical response of the rocks depends on the percentage of each phase. When the rock is matrix dominant, the electrical resistivity trend fits with the Hashin-

Shtrikman lower bound for multiphase systems (considering gypsum, anhydrite and matrix as the components). On the other hand, when the rock is calcium sulphate dominant the trend shows the one of the Hashin-Shtrikman upper bound. The reference electrical resistivity value of pure anhydrite rocks has been defined as 10^4 Ω.m and geoelectrical classification for calcium sulphate rocks has been elaborated. With this classification it is possible to differentiate between calcium sulphate rocks with different composition from their electrical resistivity value. This classification has been checked with field examples and calculating the theoretical resistivity value of thin section photographs with the program ELECFEM2D. The electrical behavior of calcium sulphate rocks is a good reference for other type of rocks with electrically differentiated components, and similar methods can be used to define their geoelectrical responses.

Keywords: Gypsum, Anhydrite, Sulphate, Electrical Conductivity

1. INTRODUCTION

Evaporites are sedimentary rocks originated from evaporation of salty water. Sulphates are one of the principal groups of evaporitic rocks and the principal sulphate minerals are: gypsum ($CaSO_4 \cdot 2H_2O$), anhydrite ($CaSO_4$), glauberite ($Na_2Ca(SO_4)_2$) and thenardite (Na_2SO_4) (Warren, 2006). Texturally, sulphate rocks are mainly crystalline; but may appear with clastic textures when they are reworked. They retain only a reduced primary porosity (<1%), display a restricted mineralogical (and geochemical) composition and can appear combined with a lutitic matrix (mainly composed of clay and microcrystalline carbonates). The texture of rocks are affected extensively by diagenetic processes which can become microcrystalline. Gypsum tends to transform to anhydrite when buried as a result of dehydration, and the opposite process also takes place when anhydrite is affected by weathering and superficial waters (Holliday, 1970).

Gypsum deposits are exploited for industrial purposes. It is mainly used in construction as drywall and as an ingredient for plaster, but it is also used in other industries (Bustillo et al., 2001). Gypsum quarries occur worldwide, with the USA and Iran as the largest producers. One of the most important problems found while quarrying gypsum is the presence of anhydrite. By comparison with gypsum, anhydrite is harder and denser. The drilling machines can be damaged by anhydrite bodies. Hence, the exploitation must be stopped immediately. Anhydrite is also used by industry for different purposes, but because of the exploitation difficulties it is mainly obtained by dehydration of previously extracted gypsum. Anhydrite (from gypsum dehydration) is commonly found deeply buried (up to 1000 m; Shearman, 1985; Warren, 2006). It rarely crops out because it tends to hydrate and transform into gypsum.

Geoelectrical techniques are proposed as a tool for studying these sulphate deposits. Electrical resistivity tomography (ERT) is a geophysical technique which can be used to obtain an image of the electrical resistivity distribution of the subsurface. For this purpose an array of metal electrodes are planted in the soil and the difference of electrical potential is measured between pairs of them while a direct current (DC) is passed between two others. The arrangement of these 4 electrodes depends on

66 the electrical array that has been selected and the measurement is repeated along the string of
67 electrodes at different spacings and positions. The apparent resistivity values obtained are inverted into
68 resistivity values as a function of depth and position using inversion software (RES2DINV, Geotomo
69 Software, ver. 3.5). This method is a rapid, non invasive and relatively low-cost.

70 Gypsum deposits have been successfully identified with ERT profiles (Lugo et al., 2008;
71 Guinea et al., 2009; Guinea et al., 2010a). Guinea et al. (2010b) produced a geoelectrical classification
72 of gypsum rocks establishing a direct relation between their electrical resistivity value and the
73 percentage of lutitic matrix (Table 1). In that study the anhydrite phase was not considered, but this
74 mineral very often appears in gypsum rocks. The scientific literature shows anhydrite to have a large
75 range of resistivities from <100 to 10^{10} Ω.m (Table 2; Jakosky, 1950; Parkhomenko, 1967; Rider,
76 1986; Robison and Çoruh, 1988; Choteau et al., 1997; Asfahani and Mohammad, 2002; Lugo et al.,
77 2008). The variation in the electrical resistivity value of anhydrite in these publications is related to the
78 presence of gypsum, but the influence of the lutitic matrix is not mentioned.

79 The aim of this study is to measure the electrical resistivity of pure anhydrite at zero frequency
80 and to establish the effect of compositional variations in the gypsum-anhydrite-lutite rock system. This
81 problem will be studied from three different angles, namely numerical modeling, laboratory
82 measurements and field data. The information thus obtained should help to interpret geoelectrical data
83 in future surveys on sulphate rocks.

84

85 **2. FIELD DATA**

86 *2.1 Geological setting*

87 During the Lutetian (Middle Eocene) a large marine evaporitic sequence was deposited in the
88 South Pyrenean Foredeep (Rosell and Pueyo, 1997). In the La Garrotxa area (eastern Pyrenees)
89 secondary gypsum (as product of the hydration of anhydrite) crops out extensively and anhydrite has

been found in borehole logs with other evaporitic rocks such as halite (Carrillo, 2009). Close to the village of Beuda (Girona, Spain) there is a quarry in which gypsum has been exploited since at least the 1930s. There are many sculptures made of alabaster (pure secondary microcrystalline gypsum) from the Middle Ages for which geochemical analysis has demonstrated that they were extracted from the Beuda gypsum unit (Inglés et al., 2009).

Nowadays the quarry has been largely developed and anhydrite crops out in many places and where the exploitation has consequently been stopped. The gypsum of the Beuda unit was produced by hydration of anhydrite and therefore there are still some anhydrite relict bodies embedded in the gypsum. In the walls of the quarry it is possible to observe boundaries between gypsum and anhydrite usually displaying a quite pure anhydrite core and a transition to pure gypsum (Figure 1A). The purity of the calcium sulphate varies from higher than 90% to close to 75% in certain layers (Figure 1B). The changes in the purity of both gypsum and anhydrite rocks and the complex geometrical relations between them make these deposits very heterogeneous. In some cases matrix bearing gypsum appears in contact with pure anhydrite and in other cases the anhydrite does not appear as a body but as fragments embedded in gypsum and filled with gypsum veins (Figure 1C). In other places anhydrite appears massive with little gypsum within (Figure 1D). Three ERT profiles (figure 2, A, B, and C) have been performed in the Beuda gypsum quarry. Profile D (Figure 2D) has been performed in the same formation of the Beuda quarry, close to the village of Serinyà. In the area studied there are sulphate layers under a soil. In the nearby outcrops pure secondary gypsum appears, but at depth, the sulphates probably transform into anhydrite as it has been observed in the region (Carrillo, 2009).

Marine evaporitic deposition took place during the upper Eocene on the Catalan margin of the Ebro basin (Ayora et al., 1994). The Odena gypsum unit was extensively exploited during the 20th century and there are many abandoned quarries in the region. Profile E has been carried out in an abandoned quarry near to the village of Odena where anhydrite crops out (Figure 2E).

In the Montes de Torrero area (Zaragoza, Spain) there is a Miocene evaporitic formation hundreds of meters thick. The area has been studied by means of boreholes in which gypsum,

anhydrite, glauberite and halite were found among other minerals. This formation has a large quantity of matrix in every layer (Ortí, 2000; Salvany, 2009). The outcropping materials are mainly gypsum, which formed from the hydration of anhydrite or glauberite (Figure 1E), and more than 50% matrix (composed of clay and marl). An ERT survey has been performed where borehole B4 was drilled (Figure 2F). The log of the borehole shows gypsum to a depth of 35 m, then glauberite to a depth of 69 m followed by anhydrite to 80 m with some interbedded layers of halite or glauberite (Salvany, 2009). The whole log shows significant fractions of matrix at all depths as such as at the surface.

2.2 Methods

A total of six ERT profiles have been carried out at anhydrite rock deposit areas in the South Pyrenean Foredeep and Ebro Basin (North East of Spain; Figure 3). The examples are presented below starting with those performed in quarries (Figure 3; A, B, C and D) and afterwards in areas with no evaporites that crop out (Figure 3; E and F). All the profiles performed in quarries show a high fraction of sulphates and therefore relatively high electrical resistivity values.

A Syscal Pro Switch ERT system with 48 electrodes and an external power supply has been used to carry out the data acquisition. The electrode spacing for the measurements in quarries was 0.5, 1.5 or 2 m depending on the local conditions. In the profiles performed where no evaporates crop out, the electrode spacing was 10 m to increase the depth of investigation because anhydrite deposits tend to appear below other formations (because at shallow depth they transform into gypsum). The used electrodes for the data acquisition were made of stainless steel and they were nailed in the terrain by means of hammers. There are many possible array configurations in geophysical prospection (Ma et al., 1997; Furman et al., 2003; Szalai and Szarka, 2008) which may be applied to anhydrite rocks. The Wenner-Schlumberger and Dipole-Dipole arrays have been selected depending of the structure under study, and the Dipole-Dipole has been used were lateral electrical resistivity changes are important. The apparent resistivity data of performed ERT profiles has been inverted with the RES2DINV program; that is available from 1995 (Loke and Barker, 1996). The inversion process has been carried out with 5 iterations for each profile. With this number of iterations the data converges in all cases

achieving an acceptable RMS error. Additional iterations do not vary the RMS error significantly but increase the electrical resistivity value in the low sensitivity areas (i.e., the pure sulphate rocks). As explained later in Section 2.3, the resistivity range calculated (with 5 iterations) in pure anhydrite bodies at depth is alike to the apparent resistivity measured in shallow pure anhydrite rocks.

Sulphate samples have also been collected in some of the profiled areas in order to measure their composition. The samples have been powdered and 0.5 g from each one has been dissolved in 250 ml of distilled water in accordance with the solubility of calcium sulphate in water. The solutions were shaken for 24 hours at 25 C^{o} and then filtered. The residue left after filtering correspond to the non-soluble phases, which are made up of the lutitic matrix (including carbonates, quartz and other minor accompanying minerals). The residue was weighted in order to estimate the fraction of the in sulphate phases.

2.3 Results and discussion

In the Beuda quarry some different areas have been studied. The profiles A and B have been performed upon areas in which massive anhydrite was found and afterwards was buried under quarry waste materials. The profiles were spread above the infilling. The result of the inversion for Profile A (Figure 3A) display an upper part with relatively low electrical resistivity values (between 10 and 200 Ω.m), which corresponds to the quarry waste. Underlying these materials there is a homogeneous body with high resistivity value (up to 10^4 Ω.m), which has been interpreted as pure anhydrite (Lugo et al., 2008). In the case of Profile B, which was performed perpendicularly to Profile A, the inverted resistivity section (Figure 3B) displays a lateral electrical resistivity variation below the quarry waste layer. A well was drilled in the middle of profile B and high hardness was found at 6 meter depth, but no core was recovered. This hardness has been interpreted as anhydrite rock with certain quantity of matrix.

The profile C has been measured in other location where anhydrite had also stopped the exploitation of the quarry. The electrodes were inserted almost directly into the sulphate rocks and

both anhydrite and gypsum appeared in the ground surface. In the inverted resistivity section (Figure 3C) there is displayed a lateral variation of electrical resistivity ranging from 10^3 to 10^4 Ω.m. The larger resistivity values are limited with the outcropping of massive anhydrite, while the lower ones are related to the presence of gypsum, and the intermediate values correspond to the transition between the two pure phases.

Profile D has been performed in an abandoned quarry near to the village of Odena where anhydrite crops out. The inverted section (Figure 3D) shows electrical resistivities ranging from 10^3 to 10^4 Ω.m, similarly to the observations in the Beuda quarry. In the areas in which the value is larger, massive anhydrite is observed. Lower electrical resistivity than 500 Ω.m are related to lutitic sedimentary layers.

Profile E has been performed in an evaporitic basin with no outcrops. The inversion of the profile (Figure 3E) displays a shallow deposit with a low electrical resistivity value (50 Ω.m) which corresponds to the underlying materials. Below this layer there is a high resistivity body ranging from 1000 to more than 5000 Ω.m and with a more conductive structure in the central part (between 100 and 200 Ω.m). This structure represents a fault present in the area, and identified on the surface by geological evidence (Carrillo, 2009).

The profile F performed in Montes de Torrero area has been modified from Guinea et al. (2010b). In the inverted image (Figure 3F) the whole deposit shows a general trend of 30-50 Ω.m with some bodies slightly more resistive (up to 300 Ω.m at the most resistive points). Those bodies would represent a higher grade of the deposit (up to 60% in sulphates) in these zones, this grade changes are related to primary depositional processes and they are very common in these materials (Guinea et al., 2010a). In any case it is not possible to differentiate between anhydrite and gypsum layers because the electrical behavior of the deposit is dominated by the abundant matrix.

As general trend, sulphate rocks with high purity in anhydrite show an electrical resistivity value up to 10^4 Ω.m after the inversion (Lugo et al., 2008). This value is considered to be the reference

for pure anhydrite rocks because in some profiles in which some of the shallowest points have been measured almost directly above massive anhydrite rocks, show an apparent resistivity value larger than 5000 Ω.m. In these cases the apparent and the inverted resistivities are similar but a slightly lower for the apparent resistivity because the electrodes are inserted into a thin clay layer. When these rocks are mixed with gypsum forming pure sulphate rocks with both phases, which are the most common in the quarries, they display an intermediate value of resistivity ranging from 1500 to 5000 Ω.m depending on the quantity of each phase. As the distribution of the anhydrite in the gypsum deposits is very heterogeneous due to the rehydration processes, the tomography lines show heterogeneous bodies with different electrical resistivity values and transitional zones. Values close to 1000 Ω.m are related to the purest gypsum rocks or to pure anhydrite with a significant quantity of matrix rocks. When the matrix has a large volume fraction, it is not possible to differentiate is gypsum from anhydrite with ERT. In these cases, the rocks will display a resistivity below 100 Ω.m, which is significantly lower than the resistivity of sulphate-rich deposits. The low electrical resistivity of sulphate deposits with large matrix volume fraction was studied further by Guinea et al. (2010b) for the case of gypsum rocks (without anhydrite).

3. LABORATORY MEASUREMENTS

3.1 Methods

Many authors have measured the electrical conductivity of geological materials (Keller, 1966; Lockner and Byerlee, 1985; Guéguen and Palciauskas, 1994; Glover et al. 1996; Giao et al., 2003; Rusell and Barker, 2010; among others). Guinea et al (2010b) made eleven gypsum-clay pills in different proportions with a range from 0 to 100% of $CaSO_4 \cdot H_2O$ at intervals of 10% in composition and measured their electrical conductivity. Three sets of eleven anhydrite-lutite pills and three sets of gypsum-lutite pills have been made using the same methodology, parameters and resources. The compositional error of the pills is below 1%, because the weight corresponding to the volume of each

fraction has been measured with a precision scale (Sarorius B3100S) with a resolution of 0.01 g (the pills have a total weight of 13.5 g). The pills have a cylindrical shape with a radius of 2 cm and a width of approximately 0.50 cm. The aim of these measures is to define the importance of the matrix presence in calcium sulphate rocks.

The conductivity measurement was carried out in accordance with the UNE 21-303-33 regulation (1983) with an electrical circuit in which the samples act as electrical resistance (Figure 4). The electrical power source was a laboratory DC converter power supply with switchable voltage (0–32 V) and current (0-10 A). Changes in the amperage above 1 A do not affect the measurements so an output current of 2 A has been selected. In order to measure the amperage of the electrical current after traversing the resistance (the sample), an analogue microammenter (Demestres 540) with a range of 0-100 μA and an accuracy of 1 μA, or a nanoammeter (Monroe 285) with a range of ±200 nA, a 0.1 nA resolution and an accuracy of 2% have been used. The potential difference is measured by a voltmeter (MY-67) with a resolution of 0.001 V connected to both sides of the pills.

The electrodes used on the samples are made of stickers with metallic buttons such as those used for electrocardiograms (Compex). The button has a conductive gel on the sticking side, forming a 0.75 cm-radius circled face (which will be considered the surface of the electrode). This gel is connected directly to the samples. The pills and the electrodes are situated above a paperboard insulator. The barrelling effect is low because the distance between the electrodes is relatively small (approximately 0.50 cm) and can be neglected. Due to the difference between the area of the electrodes and the area of the pills, there is a leak path for the electrical current (Roth, 1959). The measurements were made after the reading stabilizes (10 seconds after the power supply is switched on). Polarization causes errors after a certain time in the pills with large fractions of clay. Hence, measurements made after current has flowed for a long time are not considered representative for geophysical surveys because geoelectrical methods use a short current injection time. Each pill has been measured three times, making a total of 6 measurements for each volume fraction. Ohm's law can be applied to calculate the conductivity (σ) or resistivity (ρ) of the sample for a known current density (j) and field (E) (Eq. 1):

244 $$j = \sigma E = E/\rho$$

245 It is possible to measure the resistance (*R*) of the samples. As the thickness (*L*) of the sample
246 and the surface area of the electrode (*S*) are known, the electrical resistivity (ρ) can be calculated (Eq.
247 2):

248 $$R = \rho \, {}^{L}/_{S}$$

249 *3.2 Results and discussion*

250 The resistivity calculated for the gypsum-lutite and anhydrite-lutite pill sets is shown in Figure
251 5 (a full measurements table is shown in Annex 1). The mean resistivity is indicated by symbols
252 together with an error bar representing the standard deviation. The measurements performed on
253 gypsum-lutite pills showed a similar trend to the one presented by Guinea et al. (2010b). The pills
254 ranging from 70 to 100% in gypsum fraction were more accurate in the present study because the
255 current was measured with a nanoammeter instead of a microammeter. The pills ranging from 0 to
256 40% in gypsum fraction displayed a slightly increasing trend of the electrical resistivity (with a mean
257 value ranging from 6 to 33 Ω.m). The 50 and 60% gypsum fraction pills displayed a transitional range
258 of resistivity (with mean values of 72 and 137 Ω.m respectively). Finally, the pills with a volume
259 fraction of gypsum ranging from 70 to 100% displayed a resistivity of >700 Ω.m. The trend shown by
260 the anhydrite pills is similar to the one shown by the gypsum pills for the case of pills with a sulphate
261 fraction from 0 to 50%. There are slight differences between them, but both sets are in the same range
262 of resistivities. The anhydrite-pills with a sulphate fraction of 60% or above are noticeably more
263 resistive than their equivalent in gypsum pills (ranging from 1012 to 7609 Ω.m mean resistivity).

264 It is evident that the grades below 60% are dominated by the lutitic matrix and the sulphate
265 component affects the measurement negligibly. The sulphate volume fractions above 70% showed
266 high resistivity values in which the dominant component is the sulphate phase. Between the two
267 differentiated trends there is a transitional zone which represents the loss of the connectivity of the

matrix. As in the measurements of the gypsum pills by Guinea et al. (2010b), the pills with a large quantity of clay component polarize with measuring time. The chargeability of clay has been widely described before (Takakura, 2006; Deucester and Kaufmann, 2009).

Percolation theory states that in a cluster with a component randomly distributed (meaning the lutitic matrix for this case) there is a percolation threshold which represents the minimal quantity of the component required in order to obtain a long-range connectivity (Stauffer and Aharony, 1985). This theory has been widely used to predict characteristics of rocks as the connection of their porosity or fractures (Karmakar et al., 2003; Wang et al., 2007). When the fraction of the component is below the percolation threshold, the cluster is not considered to be connected. In our system the percolation is controlled by conduction through matrix which is much more conductive than the sulphate phase. Anhydrite or gypsum components are dielectric (act as resistances) and they conduct little electrical current while the matrix fraction is above the percolation threshold. Below the percolation threshold, the electrical current finds no connected pathways in the matrix and passes through the sulphates. Hence, the relative proportion of gypsum and anhydrite phases when the presence of matrix is above 40%, do not affect the electrical resistivity value of the whole rock.

4. THEORETICAL CALCULATIONS

4.1 Methods

Physical properties of rocks are mainly functions of their microstructure (Guéguen and Palciauskas, 1994). Two important mathematical approaches are effective medium theory (EMT) and percolation theory. The EMT (Kirpatrick, 1973) approximation is quite good for rocks with quasi-uniform distributions where only a small degree of heterogeneity is observed, although they cannot describe correctly the phenomenon of clustering (Guéguen et al., 1997) when the heterogeneity is large. Moreover, the knowledge of the geometric distribution and connectivity of the minor phase is of great importance. Percolation theory describes the medium in terms of probabilities of the connectivity

but does not provide bulk physical properties. Here, we propose a method to determine the physical properties of composite materials that combines the EMT and the percolation theory. On one hand, the EMT is used to calculate the bounds of the physical properties depending on the amount of the matrix phase present. These limits correspond to the two extreme situations where the matrix phase is totally interconnected or disconnected. On the other hand, the percolation theory is used to determine the probability of having a connected or interconnected matrix phase assuming that it is distributed in a single cube distribution.

The effective properties of composites, in particular electrical conductivity, have been studied analytically for a long time for a very simple cases (i.e., Maxwell (1881) used effective medium theory to derive the bulk conductivity of spheres dispersed in a continuous medium). The rocks can be considered as random materials of different property phases at various length scales. To compute the effective properties of such materials requires knowledge of the microstructure and require numerical computation. Garboczi (1999) wrote an algorithm and the consequent FORTRAN code to compute using both finite difference and finite element codes to calculate the electrical an elastic effective properties of materials with different phases from digital images.

In this paper the program ELECFEM2D.F from Garboczi (1999) has been used to compute the effective conductivity of gypsum-anhydrite rock samples. The method to calculate the electrical conductivity of these rocks is to analyze thin section images in which the amount of both anhydrite and gypsum proportion together with the one of the lutitic matrix is known. With this software it is possible to obtain a resistivity distribution model based on a microphotograph.

In order to perform the theoretical calculation of photographs with the program ELECFEM2D.F, the pictures must be converted from an image format file (e.g., JPG, JPEG, GIF, PNG) into an ASCII file. This has been carried out with a converter which creates numerical files from the pixels of the input image. Depending on the color range of these pixels, a numeric value, which is related to a user defined electrical resistivity value, is assigned. As the images used display lutite, gypsum and anhydrite phases; 10, 10^3 and 10^4 Ω.m electrical resistivity values have been selected

319 respectively. This selection will be discussed further in Section 4.2. The number of variables is user
320 defined and 2 variables (1 and 2) have been selected for photographs displaying 2 phases (any couple
321 of lutite-gypsum-anhydrite) and 3 variables (1, 2 and 3) when the 3 of them are present. Each image
322 was previously treated with an image processing program in order to homogenize the colour ranges in
323 order to improve the detection of each phase.

324 Once the ASCII file is created, it can be used by the ELECFEM2D.F program. The program
325 divides the surface into 8400 (150×56) cells with an electrical resistivity value assigned to each one,
326 and calculates the current intensity remaining after crossing the system in the *x* or *y* direction. Both
327 directions and the arithmetic mean value have been calculated; the differences are related to the
328 anisotropic distribution of the phases. The selected potential gradient was set to 1 V/m.

329 *4.2 Mixing models for two and three phase systems*

330 Many mixing models have been published in order to predict the bulk conductivity of a porous
331 medium (Glover et al., 2000). In the case of sulphate rocks there is no porosity; hence, the resistivity
332 (or conductivity) of the bulk rock depends on the fraction (γ) and the electrical resistivity value (ρ) of
333 each component and on the connectivity and geometrical distribution of the matrix (which has the role
334 of a conducting fluid in a saturated porous medium). Different mixing models (Parallel, Perpendicular,
335 Random, Modified Archie's law and Hashin Shtrickman bounds) have been calculated for the case of
336 two-phase sulphate rocks (gypsum-lutite and anhydrite-lutite) with different proportions of sulphate
337 and matrix. The electrical resistivity values selected for gypsum and lutite phases have been 10^3 and
338 10 Ω.m, respectively (Guinea et al., 2010b). The electrical resistivity value selected for pure anhydrite
339 phase has been 10^4 Ω.m, in accordance with the maximum value measured in field examples and the
340 bibliography (Table 2).

341 Parallel and Perpendicular mixing models (Table 3A and B; Somerton, 1992; Guéguen and
342 Palciauskas, 1994) describe the conductivity of a layered distribution of phases with a constant
343 arbitrary thickness arranged axially or normally (in each case) to the current flow. The random model

(Table 3C; Warren and Price, 1961; Shankland and Waff, 1977) describes the bulk conductivity of a material with randomly distributed arbitrary volumes of the conductive phase. Glover (2000) described a mixing model (Table 3D) derived from Archie's law (Archie, 1942), considering the boundary conditions implied by geometrical constrains. To calculate this model, the cementation exponent *m* has to be defined for each phase. This variable depends on the connectedness of the phases and, as long as in the present case there is no information about this connectedness, it has been tested with different values of *m* to adjust the data. When the matrix is dominant, *m*=0.25 is consistent with the data obtained for both anhydrite and gypsum pills, which indicates that the structure of the matrix is the same for both types of sample. In the case of pills with higher sulphate fractions, *m*=0.01 and *m*=0.006 has been selected for gypsum and anhydrite pills respectively. Hashin and Shtrikman (1963) defined the electrical resistivity value bounds (HS bounds) of a bulk rock from effective medium considerations. These bonds represent the theoretical maximum (upper bound; Table 3E) and minimum (lower bound; Table 3F) electrical resistivity value that any material formed of two different phases with a certain fraction can display.

The mentioned mixing models are displayed in the Figure 6 for both gypsum-lutite (Figure 6A) and anhydrite-lutite (Figure 6B) systems. Additionally to the theoretical trends of the mixing models, the resistivities calculated in the laboratory measurements are displayed. The pill samples with a fraction of sulphate phases of 50% or below show a similar trend to the one displayed by the HS^- model. This is also shown in the field data in the profiles in which the sulphate formations have a high quantity of matrix within. On the other hand, the resistivity of the pills with a sulphate fraction of 70% or above is closer to the perpendicular or HS^+ models. In the case of the anhydrite pills with high sulphate fraction, they fit better to the random model; but this can be related to the fact that the anhydrite pills are slightly watered during their elaboration. The modified Archie's law also fits well to the laboratory data; the two different trends (low sulphate fractions and high sulphate fractions) have been bridged by means of variations of *m* in their end ranges (showed as dashed lines in the graphic). The field data obtained in anhydrite rocks indicate that the observed resistivity ranges fit better to the perpendicular or HS^+ models. The values obtained for the pills with 60% in sulphate

fraction are transitional, which represents the percolation threshold. Theoretically the percolation threshold occurs in a single phase fraction but in the case of real rocks transitional values are displayed in this range of composition.

From the trends observed for these two-phase systems, it can be considered, as approximation, that the HS bounds define the resistivity of gypsum and anhydrite rocks depending on the quantity of matrix present (modified Archie's law is also a good approximation, but the value of *m* has to be defined). When the matrix is percolating (sulphate fraction of 50% or below), the resistivity of the sulphate rocks is bounded to the HS^- model. In the case of non percolating matrix (sulphate fraction of 70% or above), the resistivity is bounded to the HS^+ model. A general form of the bounds for *n*-phases was given by Berriman (1995). With his formula it is possible to construct a ternary graphic for 3-phased rocks (Ledo and Jones, 2005). The gypsum-Anhydrite-Lutite (GAL) system has been calculated for both upper (Table 3G) and lower (Table 3H) HS bounds. In the case of lower bound (Figure 7A), the system is clearly dominated by the lutitic component; the isoresistivity lines are parallel between them showing no appreciable variation in the gypsum-anhydrite axis but when the lutite fraction is less than 10%. The values of resistivity are very low in general, showing less than 100 Ω.m for a sulphate fraction of 70%. The upper bound (Figure 7B) displays a very different trend dominated by the anhydrite fraction, but in this case the 3 components affect the bulk resistivity value of the rock. The electrical resistivity values are much larger than in the case of lower bound achieving 1000 Ω.m with only 40% of anhydrite. As it has been previously shown, the electrical behavior of the rocks is the one of lower HS bound when the quantity of sulphate is of 50% or below and the one of upper bound when is of 70% or above. Thus it is expected that the real distribution of the electrical resistivity for the GAL system should be a combination between the upper and lower HS bounds (Figure 7C).

4.3 Results and discussion

In order to check the accurateness of this GAL diagram, the theoretical electrical resistivity value of real thin section rock photographs (Figure 8) has been calculated with ELECFEM2D

program. Lutitic matrix display brownish colouring while both anhydrite and gypsum have are transparent underplane polarized light; having anhydrite higher relief than gypsum (its bounds are well marked with dark lines). With crossed polarized light, gypsum and anhydrite can be easily differentiated because of the different coloring of the anhydrite (pink, green, blue) in contrast with the gray colors of the gypsum crystals. The standard electrical resistivity values selected for the gypsum, anhydrite and lutitic matrix phases have been 10^3, 10^4 and 10 Ω.m respectively, as has been assigned before. The electrical resistivity of the bulk sections has been measured in both *x* and *y* directions; when the distribution of the components is homogeneous these values would be considered similar. For each thin section the fractions of the components are calculated by the program so it is possible to obtain the electrical resistivity value corresponding to these fractions calculated with different mixing models (Table 4). Modified Archie's law has not been calculated for the case of 3-phase system because it would require writing and implementing a numerical inversion program to calculate *m* and *p* in function of the volume fraction, which is not the aim of this article.

The results show that the mean of the calculated electrical resistivity values in *x* and *y* directions are in general close to HS^+ bound when the fraction of sulphate is 70% or higher (Figure 8, thin sections A, D, E, F, G and H; Table 4) and to the HS^- bound when the fraction of matrix is abundant (Figure 8, B and I; Table 4). There is a good match between the corresponding position of each sample in the figure 7C, according to their components percentages, and the calculated resistivity values. In the case of thin sections C and J there is abundant matrix (58 and 52% respectively); nevertheless, the calculated resistivity values are slightly larger than that expected for such mixture. This is due to that the phases are not scattered and randomly distributed within the samples but forming compact and pure areas. This represents large heterogeneities which change the percolating behavior (we have considered it only for regular distributions of the phases as in the case of the pills) of the bulk rock and makes the transition zone larger. In any case the values are always much closer to the lower bound that to the upper one. The parallel and perpendicular (series) models do not fit well to the calculated resistivities. The random model fits well in many cases but in samples with large fraction of anhydrite, calculated resistivity is too high (especially in C thin section).

At larger scale (as in the ERT profiles) the rocks are in general more homogeneous and should fit to the HS lower bound for compositions of 0-60% in lutitic matrix. The microscopic anisotropies do not affect to the electrical conductivity of the bulk deposit if we increase the scale. In any case, it is possible to observe cases of heterogeneities at metric scale. When these heterogeneities are large, they can be considered as different rocks (for example a gypsum-rich lutite body within a larger pure gypsum host-rock). In any case, heterogeneities below the detection limit of the method will be considered as a single rock. Another possible case is a layered deposit in which every layer has different purity in the sulphate phase. If the difference among grades is low, which is the most common case, the whole sequence can be considered as a single member with a mean grade. Rarely sulphate deposits have great variations of grade from layer to layer forming a heterogeneous sequence. Sudden variations in the grade exist, but are normally associated with the limit of a sequence or a stable change in the depositional conditions. In the case of having layering between almost pure matrix and highly pure sulphates, the transitional values of resistivity will increase their range as happens in the case of the microphotographs.

5 GEOELECTRICAL CLASSIFICATION OF CALCIUM SULPHATE ROCKS

With the GAL diagram obtained combining both HS^+ and HS^- boundaries for a gypsum anhydrite-lutite system (Figure 7C) a geoelectrical classification has been elaborated differentiating 6 calcium sulphate rock types (Figure 9). When the lutitic matrix is connected at long range (in the case of sulphate fraction of 50% or below) the system is matrix dominant and therefore there is no possibility of differentiating between gypsum and anhydrite components; these rocks are classified as lutites and gypsum/anhydrite rich lutites. The electrical resistivity of this groups range from 10 to 100 Ω.m. When the sulphate grade is of 70% or above, the rock will be considered as pure gypsum when it ranges from 700 to 1000 Ω.m as was stated by Guinea et al. (2010b) for the case of gypsum-lutite systems. If the sulphate mineral is mainly anhydrite (more than 90%) the rock is considered pure anhydrite and its electrical resistivity value range from 2500 to 10^4 Ω.m depending on the rock grade.

In the case of presence of both gypsum and anhydrite sulphate phases, the rock is considered gypsum with anhydrite (1000 to 2000 Ω.m) or anhydrite with gypsum (2000 to 5000 Ω.m). The values of pure anhydrite and anhydrite with gypsum overlap; in this case it is possible to bond the electrical value to pure anhydrite rocks when there is no evidence of rehydration and to the anhydrite with gypsum otherwise. Between lutites and gypsum/anhydrite rich lutites and the sulphate pure rocks there is a transitional area displaying transitional values from 100 to 700-2500 Ω.m (depending on the sulphate composition). The lower boundary of Transitional gypsum/anhydrite rocks has been selected as 55% in sulphate fraction instead of 60% because the measures in pills have shown that the 60% values display an electrical resistivity increasing trend; the upper boundary is 70% in gypsum fraction. This transitional area is displayed with a resistivity-trend calculated by interpolation between lower and upper HS bounds, but the resistivity in the transition zone is uncertain and therefore the displayed trend is only a reference.

For the microscopic scale, it has been shown that the transitional range is wider (including rocks between 55 and 70% in sulphate fraction, depending of the anisotropy). For the cases of sulphate fractions of 55% or below or higher than 70%, the values obtained are similar to the corresponding HS bound. At larger scale, the ERT lines have shown relationships between composition and resistivity values similar to the ones displayed in the classification of the Figure 9; that is, higher than 5000 Ω.m when the dominant phase is the anhydrite, 1500 to 5000 Ω.m for different proportions of gypsum and anhydrite (with presence of little lutite) and close to 1000 Ω.m when the gypsum is the dominant phase. For deposits with large amount of lutites, the obtained value has been <60 Ω.m in all cases.

6. CONCLUSIONS

The electrical properties of calcium sulphate rocks have been widely studied at different scales with microphotographs, synthetic pills and geological deposits. Laboratory tests in pills have shown that the matrix of calcium sulphate rocks may be affected by the percolation phenomena and therefore,

when the sulphate fraction in a rock is of 55% or below, the matrix controls the resistivity of the bulk rock. When the sulphate fraction is of 70% or above, the sulphate minerals control the electrical resistivity of the bulk rock.

The electrical resistivity value of anhydrite rocks range from 10 to 10^4 Ω.m, being larger in the purest anhydrite rocks. This value is found in the field examples where the anhydrite appears in massive form. The values observed in rocks with both gypsum and anhydrite (with minor matrix) have ranged between 1500 and 5000 Ω.m depending on the quantity of each other. Large quantity of matrix in sulphate rocks have shown low electrical resistivity values been unable to differentiate between gypsum and anhydrite.

When the matrix of the calcium sulphate rocks is above the percolation threshold (i.e., more than 45%), the electrical resistivity value fits the value calculated with the Hashin-Shtrikman lower bound (HS^-), and when is embedded in the sulphate phase (i.e., 30% of matrix or less) the resistivity follows the Hashin-Shtrikman upper bound (HS^+). If there are large heterogeneities in the distribution of the phases, the resistivities of rocks with a matrix quantity ranging from 30 to 45% can display transitional values (more than 100 Ω.m, without reaching values of the purest sulphate rocks). Therefore, it is possible to calculate any combination of these 3 components and the geoelectrical classification has been elaborated for calcium sulphate rocks. With this classification is possible to determine the purity of the sulphates and the presence of anhydrite in gypsum rocks, which is useful for the characterization of the deposit.

ACKNOWLEDGEMENTS

The present work is a part of a PhD thesis supported by the "Programa General d'Intensificació de la Recerca" (Generalitat de Catalunya-UB) and the Spanish Government Projects CGL2009-11096, CGL2009-07025, CGL2010-18260 and CGL2009-07604. We want to appreciate the support and facilities of Dr. Albert Casas (Universitat de Barcelona, UB) and Dr. Ricard Bosch

(Universitat Politècnica de Barcelona, UPC). We also want to thank the reviewers of the paper for their interesting comments and particularly to Dr. Paul Glover (University of Leeds) for his detailed review. Finally we want to appreciate the support of Grupo Uralita Corporation, especially to Ms. Mayte Martín, for letting us work in the quarry of Beuda and for their support.

REFERENCES:

Asfahani, J., Mohamad, R., 2002. Geo-electrical investigation for sulphur prospecting in Teshreen Structure in Northeast Syria. Exploration and Mining Geology, 11, 49-59.

Archie, G.E., 1942. The electrical resistivity log as an aid in determining some reservoir characteristics. Transactions of the American Institute of Mining, Metallurgical, and Petroleum Engineers, 146, 54-62.

Ayora, C., García-Veigas, J., Pueyo, J.J., 1994. The chemical and hydrological evolution of an ancient potash-forming evaporite basin as constrained by mineral sequence, fluid inclusion composition and numerical simulation. Geochimica et Cosmochimica Acta, 58, 3379-3394.

Berriman, J.G., 1995. Mixture theories for rock properties. In: T.J. Ares Ed., Rock Physics and Phase Relations: A Handbook of Physical Constants. American Geophysical Union, Washington, 236pp.

Bustillo, M., Calvo, J.P., Fueyo, L., 2001. Rocas Industriales: Tipología, aplicaciones en la construcción y empresas del sector. Rocas y Minerales (ed.). 410pp.

Carrillo, E., 2009. Unidades evaporíticas eocenas de la Zona Surpirenaica Oriental (Área de La Garrotxa). Geogaceta, 47, 73-76.

Chouteau, M., Phillips, G., Prugger, A., 1997. Mapping and monitoring softrock mining. In: Proceedings of Exploration 97: Fourth Decennial International Conference of Mineral Exploration, A.G. Gubins Ed., 927-940.

Deucester, J.& Kaufmann, O., 2009. Correlation between inverted chargeabilities and organic compounds concentrations in soils-A field experiment. 15th Near Surface meeting, Dublin, Ireland, Expanded Abstracts, C19.

Furman, A., Ferré, P.A., Warrik, A.W., 2003. A Sensitivity Analysis of Electrical Resistivity Tomography Array Types Using Analytical Element Modeling. Vadose Zone Journal, 2, 416-423.

Garboczi, E.J., 1999. Finite element and finite difference programs for computing the linear electric and elastic properties of digital images of random materials. NIST Internal Report 6269. Also available at http://ciks.cbt.nist.gov/garbocz/

Giao, P.H., Chung, S.G., Kym, D.Y., Tanaka, H., 2003. Electric imaging and laboratory resistivity testing for geotechnical investigation of Pusan clay deposits. Journal of Applied Geophysics, 52, 157-175.

Glover, P.W.J., Gomez, J.B., Meredith, P.G., Boon, S.A., Sammonds, P.R., Murrell, S.A.F., 1996. Modelling the Stress/Strain Behaviour of Saturated Rocks Undergoing Triaxial Deformation using Complex Electrical Conductivity Measurements, In Integrated Experimental Measurements and Theoretical Modelling of Rock Transport Properties. Surveys in Geophysics, 17, 307-330.

Glover, P.W.J., Hole, M.J., Pous, J., 2000. A modified Archie's law for two conducting phases. Earth and Planetary Science Letters, 180, 369-383.

Guéguen, Y., Chelidze, T., Le Ravalec, M., 1997. Microstructures, percolation thresholds, and rock physical properties. Tectonophysics, 279, 23-35.

543 Guéguen, Y., Palciauskas, V., 1994. Introduction to the physics of rocks. Princenton
544 University Press, Princenton, NJ, 294pp.

545 Guinea, A., Playà, E., Rivero, L., Salvany, J.M., Himi, M., 2009. Geoelectrical imaging
546 supporting glauberite deposits evaluation in the Montes de Torrero area (Zaragoza). Geogaceta, 47,
547 145-148.

548 Guinea, A., Playà, E., Rivero, L., Himi, M., 2010a. Electrical Resistivity Tomography and
549 Induced Polarization techniques applied to the identification of gypsum rocks. Near Surface
550 Geophysics, 8, 249-257.

551 Guinea, A., Playà, E., Rivero, L., Himi, M., Bosch, R., 2010b. Geoelectrical Classification of
552 Gypsum Rocks. Surveys in Geophysics, 31 (6), 557-580.

553 Hashin, Z., Shtrikman, S., 1963. A variational approach to the theory of the elastic behavior of
554 multiphase materials. Journal of the Mechanics and Physics of Solids, 11, 12-140.

555 Holliday, D.W., 1970. The petrology of secondary gypsum rocks: a review. Journal of
556 Sedimentary Petrology, 40, 734-744.

557 Inglés, M., Manote, M.R., Ortí, F., Pey, J., Playà, E., Rosell, L., Yeguas, J., 2009.
558 Geochemical methods in alabaster provenance: an application example. IX ASMOSIA:
559 Interdisciplinary Studies on Ancient Stone meeting, Tarragona, Spain, Abstracts 125.

560 Jakosky, J.J., 1950. Exploration geophysics. Trija Publishing Co., Los Angeles, 1195pp.

561 Karmakar, R., Manna, S.S., Dutta, T., 2003. A geometrical model of diagenesis using
562 percolation theory. Physica A, 318, 113-120.

563 Keller, G.V., 1966. Electrical properties of rocks and minerals. In: Clark S.P. (Ed.), Handbook
564 of physical constants. The Geological Society of America, 587pp.

565 Kirkpatrick, S., 1973. Percolation and conduction. Reviews of Modern Physics, 45, 574-588.

566 Klein, C., Hurlburt, C.S., 1998. Manual de mineralogía de Dana. Reverté, 438pp.

567 Ledo, J., Jones, A.G., 2005. Upper mantle temperature determined from combining mineral
568 composition, electrical conductivity laboratory studies and magnetotelluric field observations:
569 Application to the intermontane belt, Northern Canadian Cordillera. Earth and Planetary Science
570 Letters, 236, 258-268.

571 Loke, M.H., Baker, R.H., 1996. Rapid least-squares inversion of apparent resistivity
572 pseudosections by a quasi-Newton method. Geophysical Prospecting, 44, 131-152.

573 Lockner, D.A., Byerlee, J.D., 1985. Complex resistivity measurements in confined rock.
574 Journal of Geophysical Research, 90, 7837-7847.

575 Lugo, E., Playà, E., Rivero, L., 2008. Aplicación de la tomografía eléctrica a la prospección de
576 formaciones evaporíticas. Geogaceta, 44, 223-226.

577 Ma, Y., Wang, H., Xu, L.A., Jiang, C., 1997. Simulation study of the electrode array used in
578 an ERT system. Chemical Engineering Science, 52, 2197-2203.

579 Maxwell, J., 1881. A Treatise on Electricity and Magnetism. Clarendon, Oxford, 2nd edition,
580 540pp.

581 Ortí, F., 2000. Unidades glauberíticas del Terciario ibérico: nuevas aportaciones. Revista de la
582 sociedad geológica de España, 13, 227-249.

583 Ortí, F., Rosell, L., Playà, E., García-Veigas, J., 2010. Large gypsum nodules in the Tertiary
584 evaporites of Spain: distribution and paleogeographic significance. Geological Quarterly, 54 (4), 411-
585 422.

586 Parkhomenko, E.J., 1967. Electrical properties of rocks. Plenum Press, New York, 314pp.

Rider, M.H., 1986. The Geological interpretation of well logs. Blackie Halsted Press, 175pp.

Robinson, E.S., Çoruh, C., 1988. Basic Exploration Geophysics. Jonh Wiley and sons, 562pp.

Rosell, L., Pueyo, J.J., 1997. Second marine evaporitic phase in the South Pyrenean Foredeep: the priabonian potash basin (Later Eocene: Autochthonous-Allochthonous Zone). In: Busson, G., Schreiber, Ch. Eds. Sedimentary deposition in rift and foreland basins in France and Spain. Columbia University Press, New York, 358–387.

Roth, A., 1959. Hochspannungstechnik. Springer, 756pp.

Rusell, E.J.F., Barker, R.D., 2010. Electrical properties of clay in relation to moisture loss. Near Surface Geophysics, 8, 173-180.

Salvany, J.M., 2009. Geología del yacimiento glauberítico de Montes de Torrero (Zaragoza). Prensas Universitarias de Zaragoza, 72pp.

Shankland, T.J., Waff, H.S., 1977. Partial melting and electrical conductivity anomalies in the upper mantle. Journal of Geophysical Research, 82, 5409-5417.

Shearman, D.J., 1985. Syndepositional and late diagenetic alteration of primary gypsum to anhydrite. In: Schreiber, B.C., (Ed.), Sixth International Symposium on Salt, vol. 1, Salt Institute, 41-55.

Somerton, W.H., 1992. Thermal properties and temperature-related behavior of rock/fluid systems. Elsevier, Amsterdam, 257pp.

Stauffer, D., Aharony, A., 1985. Introduction to percolation theory. Taylor and Francis (Eds.), 181pp.

Szalai, S., Szarka, L., 2008. On the classification of surface geoelectric arrays. Geophysical Prospecting, 56, 159-175.

609 Takakura, S., Nakada, K., 2006. IP measurements on tunnel walls of a sericite deposit – A
610 contact method of nonpolarizable electrodes on a base rock and detection of clay minerals by
611 normalised chargeability. Geophysical Exploration, 59, 363–370.

612 UNE 21-303-83, norma española, 1983. Métodos para la medida de la resistividad transversal
613 y superficial de los materiales aislantes eléctricos sólidos. Instituto Español de Normalización.

614 Wang, K.W., Sun, J.M., Guan, J.T., Zhu, D.W., 2007. A percolation study of electrical
615 properties of reservoir rocks. Physica A, 380, 19–26.

616 Warren, J.E., Price, A.C., 1961. Flow in heterogeneous porous media. Society of Petroleum
617 Engineers Journal, 1, 153-169.

618 Warren, J.K., 2006. Evaporites: sediments, resources and hydrocarbons. Springer, 1035pp.
619

TABLE CAPTIONS

Table 1: Geoelectrical classification of gypsum rocks (modified after Guinea et al. 2010b).

Table 2: Electrical resistivity values for anhydrite rocks in the literature.

Table 3: Summary of the equations of the mixing models used in the present study (modified from Glover et al., 2000).

Table 4: Results of the theoretical calculations of electrical resistivity of the thin section photographs with ELECFEM2D software. Parallel, Series, Random, Archie's modified law and Lower (HS^-) and upper (HS^+) Hashin-Shtrikman bounds have been calculated, only considering the proportion of each phase. The calculated resistivity for each sample in both x^- and y^- directions is listed in the right column. The corresponding images of the thin sections A to J are displayed in Figure 8.

FIGURE CAPTIONS

Figure 1: Photographs of the areas studied with ERT, A to C are taken in the Beuda quarry while D is taken in the area of Odena and E in the Zaragoza formation. A) pure gypsum-anhydrite boundary with a interdigitation between them; B) sulphate layers showing less gypsum fraction than in other areas; C) anhydrite blocks filled with gypsum veins and embedded in a gypsum matrix; D) massive anhydrite body; E) impure sulphate layers in Montes de Torrero area.

Figure 2: Distribution of evaporite formations in the Tertiary basins northeastern Spain indicating the location of the nine studied ERT profiles with black dots (modified from Ortí et al., 2010).

Figure 3: Inverted electrical resistivity tomography data for the different areas studied (the locations of the profiles are shown in figure 2). Profile F modified from Guinea et al. (2010b).

Figure 4: Electrical circuit to measure the electrical resistivity of the samples. It consists of a switchable laboratory power-supply (EA-PS 3032-10B), two electrodes, a voltmeter (MY-67) and a micro- or nanoammeter depending on the samples (Demestres 540 and Monroe 285, respectively).

Figure 5: Semi-logarithmic plots representing the results of the measurements of gypsum-lutite (A) and anhydrite-lutite (B) pills. The symbols represent the mean of the calculated resistivities for each sulphate fraction (calculated from a total of 6 measurements for every fraction) and the error bar represents the standard deviation. The error on the X axis is not showed because is below 1%.

Figure 6: Different mixing models calculated for the case of gypsum-lutite (A) and anhydrite-lutite rocks (B). The dashed lines in the modified Archie's model represent the transition between the low sulphate fraction and high sulphate fraction trends. The resistivity ranges obtained in the laboratory essays (Figure 5) are superimposed for both cases.

Figure 7: Ternary plots showing Hashin-Shtrikman bounds for gypsum-anhydrite-lutite (GAL) system. A) lower HS bound; B) upper HS bound; C) combined diagram considering the percolation phenomena.

Figure 8: Microphotographs of thin sections of calcium sulphate rocks; D, E, H and I are taken with cross-polarized light and the rest with plane polarized light. The different phases are indicated with numbers 1 (gypsum), 2 (anhydrite) and 3 (lutite/carbonate).

Figure 9: Geoelectrical classification of calcium sulphate rocks, depending on their gypsum-anhydrite-lutite fraction. The resistivity values are shown in the background (Figure 7C).

ANNEX

Annex 1: Results of the laboratory measurements on synthetic pills made by mixing powdered pure anhydrite or gypsum with clay. G samples correspond to gypsum-lutite pills, while A samples correspond to anhydrite-lutite pills. Samples with a sulphate fraction of 70% or above have been

666 measured with a nanoammeter and the rest with a microammeter. The mean resistivity for each
667 fraction and the standard deviation is showed in Figure 5.

THE ELECTRICAL PROPERTIES OF CALCIUM SULPHATE ROCKS FROM DECAMETRIC TO MICROMETRIC SCALE

UNCHANGED FIRST REVISION (second revision is placed after this one)

Ander Guinea[1]*, Elisabet Playà[1], Lluís Rivero[1], Juan José Ledo[2], Pilar Queralt[2]

[1]*Departament de Geoquímica, Petrologia i Prospecció Geològica. Facultat de Geologia, Universitat de Barcelona (UB). Martí i Franquès s/n, 08028 Barcelona, Spain.*

[2]*Departament de Geodinàmica i Geofísica. Facultat de Geologia, Universitat de Barcelona (UB). Martí i Franquès s/n, 08028 Barcelona, Spain.*

E-mails: anderguinea@ub.edu; eplaya@ub.edu; lrivero@ub.edu; jledo@ub.edu; pilar.queralt@ub.edu

*Corresponding author: *Phone number: +34 934 03 11 65. Fax number: +34 934 02 14 17*

ABSTRACT

Sulphate rocks have a sedimentary evaporitic origin and are present in many deposits worldwide. Among them, gypsum (dihydrated calcium sulphate) is the most common and is exploited for industrial purposes. Anhydrite (calcium sulphate) is frequently found in gypsum quarries and in non-outcropping sulphates. The greater hardness of anhydrite compared to gypsum causes a problem for gypsum extraction; quarry fronts have to be halted as soon as anhydrite is found. In this work the electrical properties of calcium sulphates have been studied by means of geoelectrical methods.

A direct relationship between the electrical conductivity values of the calcium sulphate rocks and their lithological composition has been established with the lutitic matrix being the main controlling factor when it is well connected. When the matrix is under the percolation threshold the sulphate phases are dominant, and the electrical response of the rocks depends on the percentage of each phase. When the rock is matrix dominant, the electrical resistivity trend fits with the Hashin-

Shtrikman lower bound for multiphase systems (considering gypsum, anhydrite and matrix as the components). On the other hand, when the rock is calcium sulphate dominant the trend shows the one of the Hashin-Shtrikman upper bound. The reference electrical resistivity value of pure anhydrite rocks has been defined as 10^4 Ω.m and geoelectrical classification for calcium sulphate rocks has been elaborated. With this classification it is possible to differentiate between calcium sulphate rocks with different composition from their electrical resistivity value. This classification has been checked with field examples and calculating the theoretical resistivity value of thin section photographs with the program ELECFEM2D. The electrical behavior of calcium sulphate rocks is a good reference for other type of rocks with electrically differentiated components, and similar methods can be used to define their geoelectrical responses.

Keywords: Gypsum, Anhydrite, Sulphate, Electrical Conductivity

1. INTRODUCTION

Evaporites are sedimentary rocks originated from evaporation of salty water. Sulphates are one of the principal groups of evaporitic rocks and the principal sulphate minerals are: gypsum ($CaSO_4 \cdot 2H_2O$), anhydrite ($CaSO_4$), glauberite ($Na_2Ca(SO_4)_2$) and thenardite (Na_2SO_4) (Warren, 2006). Texturally, sulphate rocks are mainly crystalline; but may appear with clastic textures when they are reworked. They retain only a reduced primary porosity (<1%), display a restricted mineralogical (and geochemical) composition and can appear combined with a lutitic matrix (mainly composed of clay and microcrystalline carbonates). These rocks are extensively affected by diagenetic processes which can change their texture into microcrystalline. Gypsum tends to transform to anhydrite when buried because of dehydration, and the opposite process also takes place when anhydrite is affected by weathering and superficial waters (Holliday, 1970).

Gypsum deposits are exploited for industrial purposes. It is mainly used in construction as drywall and as an ingredient for plaster, but it is also used in other industries (Bustillo et al., 2001). Gypsum quarries occur worldwide, with the USA and Iran as the largest producers. One of the most important problems found while quarrying gypsum is the presence of anhydrite. By comparison with gypsum, anhydrite is harder and denser. The drilling machines can be damaged by anhydrite bodies. Hence, the exploitation must be stopped immediately. Anhydrite is also used by industry for different purposes, but because of the exploitation difficulties it is mainly obtained by dehydration of previously extracted gypsum. Anhydrite (from gypsum dehydration) is commonly found deeply buried (until 500-1000 m; Shearman, 1985; Warren, 2006). It rarely crops out because it tends to hydrate and transform into gypsum.

Geoelectrical techniques are proposed as tool for studying these sulphate deposits. Electrical resistivity tomography (ERT) is a geophysical technique which can be used to obtain an image of the electrical resistivity distribution of the subsurface. For this purpose an array of metal electrodes are planted in the soil and the difference of electrical potential is measured between pairs of them while a direct current (DC) is passed between two others. The arrangement of these 4 electrodes depends on

66 the electrical array that has been selected and the measurement is repeated along the string of
67 electrodes at different spacings and positions. The apparent resistivity values obtained are inverted into
68 resistivity values as a function of depth and position using inversion software (RES2DINV, Geotomo
69 Software, ver. 3.5). This method is a rapid, non invasive and relatively low-cost.

70 Gypsum deposits have been successfully identified with ERT profiles (Lugo et al., 2008;
71 Guinea et al., 2009; Guinea et al., 2010a). Guinea et al. (2010b) produced a geoelectrical classification
72 of gypsum rocks establishing a direct relation between their electrical resistivity value and the
73 percentage of lutitic matrix (Table 1). In that study the anhydrite phase was not considered, but this
74 mineral very often appears in gypsum rocks. The scientific literature shows anhydrite to have a large
75 range of resistivities from <100 to 10^{10} Ω.m (Table 2; Jakosky, 1950; Parkhomenko, 1967; Rider,
76 1986; Robison and Çoruh, 1988; Choteau et al., 1997; Asfahani and Mohammad, 2002; Lugo et al.,
77 2008). The variation in the electrical resistivity value of anhydrite in these publications is related to the
78 presence of gypsum, but the influence of the lutitic matrix is not mentioned.

79 The aim of this study is to measure the electrical resistivity of pure anhydrite at zero frequency
80 and to establish the effect of compositional variations in the gypsum-anhydrite-lutite rock system. This
81 problem will be studied from three different angles, namely numerical modeling, laboratory
82 measurements and field data. The information thus obtained should help to interpret geoelectrical data
83 in future surveys on sulphate rocks.

84

85 **2. FIELD DATA**

86 *2.1 Geological setting*

87 During the Lutetian (Middle Eocene) a large marine evaporitic sequence was deposited in the
88 South Pyrenean Foredeep (Rosell and Pueyo, 1997). In the La Garrotxa area (eastern Pyrenees)
89 secondary gypsum (as product of the hydration of anhydrite) crops out extensively and anhydrite has

been found in borehole logs with other evaporitic rocks such as halite (Carrillo, 2009). Close to the village of Beuda (Girona, Spain) there is a quarry in which gypsum has been exploited since at least the 1930s. There are many sculptures made of alabaster (pure secondary microcrystalline gypsum) from the Middle Ages for which geochemical analysis has demonstrated that they were extracted from the Beuda gypsum unit (Inglés et al., 2009).

Nowadays the quarry has been largely developed and anhydrite crops out in many places and where the exploitation has consequently been stopped. The gypsum of the Beuda unit was produced by hydration of anhydrite and therefore there are still some anhydrite relict bodies embedded in the gypsum. In the walls of the quarry it is possible to observe boundaries between gypsum and anhydrite usually displaying a quite pure anhydrite core and a transition to pure gypsum (Figure 1A). The purity of the calcium sulphate varies from higher than 90% to close to 75% in certain layers (Figure 1B). The changes in the purity of both gypsum and anhydrite rocks and the complex geometrical relations between them make these deposits very heterogeneous. In some cases matrix bearing gypsum appears in contact with pure anhydrite and in other cases the anhydrite does not appear as a body but as fragments embedded in gypsum and filled with gypsum veins (Figure 1C). In other places anhydrite appears massive with little gypsum within (Figure 1D). Three ERT profiles (figure 2, A, B, and C) have been performed in the Beuda gypsum quarry. Profile D (Figure 2D) has been performed in the same formation of the Beuda quarry, close to the village of Serinyà. In the area studied there are sulphate layers under a soil. In the nearby outcrops pure secondary gypsum appears, but at depth, the sulphates probably transform into anhydrite as it has been observed in the region (Carrillo, 2009).

Marine evaporitic deposition took place during the upper Eocene on the Catalan margin of the Ebro basin (Ayora et al., 1994). The Odena gypsum unit was extensively exploited during the 20th century and there are many abandoned quarries in the region. Profile E has been carried out in an abandoned quarry near to the village of Odena where anhydrite crops out (Figure 2E).

In the Montes de Torrero area (Zaragoza, Spain) there is a Miocene evaporitic formation hundreds of meters thick. The area has been studied by means of boreholes in which gypsum,

anhydrite, glauberite and halite were found among other minerals. This formation has a large quantity of matrix in every layer (Ortí, 2000; Salvany, 2009). The outcropping materials are mainly gypsum, which formed from the hydration of anhydrite or glauberite (Figure 1E), and more than 50% matrix (composed of clay and marl). An ERT survey has been performed where borehole B4 was drilled (Figure 2F). The log of the borehole shows gypsum to a depth of 35 m, then glauberite to a depth of 69 m followed by anhydrite to 80 m with some interbedded layers of halite or glauberite (Salvany, 2009). The whole log shows significant fractions of matrix at all depths as such as at the surface.

2.2 Methods

A total of six ERT profiles have been carried out at anhydrite rock deposit areas in the South Pyrenean Foredeep and Ebro Basin (North East of Spain; Figure 3). The examples are presented below starting with those performed in quarries (Figure 3; A, B, C and D) and afterwards in areas with no evaporites that crop out (Figure 3; E and F). All the profiles performed in quarries show a high fraction of sulphates and therefore relatively high electrical resistivity values.

A Syscal Pro Switch ERT system with 48 electrodes and an external power supply has been used to carry out the data acquisition. The electrode spacing for the measurements in quarries was 0.5, 1.5 or 2 m depending on the local conditions. In the profiles performed where no evaporates crop out, the electrode spacing was 10 m to increase the depth of investigation because anhydrite deposits tend to appear below other formations (because at shallow depth they transform into gypsum). The used electrodes for the data acquisition were made of stainless steel and they were nailed in the terrain by means of hammers. There are many possible array configurations in geophysical prospection (Ma et al., 1997; Furman et al., 2003; Szalai and Szarka, 2008) which may be applied to anhydrite rocks. The Wenner-Schlumberger and Dipole-Dipole arrays have been selected depending of the structure under study, and the Dipole-Dipole has been used were lateral electrical resistivity changes are important. The apparent resistivity data of performed ERT profiles has been inverted with the RES2DINV program; that is available from 1995 (Loke and Barker, 1996). The inversion process has been carried out with 5 iterations for each profile. With this number of iterations the data converges in all cases

achieving an acceptable RMS error. Additional iterations do not vary the RMS error significantly but increase the electrical resistivity value in the low sensitivity areas (i.e., the pure sulphate rocks). As explained later in Section 2.3, the resistivity range calculated (with 5 iterations) in pure anhydrite bodies at depth is alike to the apparent resistivity measured in shallow pure anhydrite rocks.

Sulphate samples have also been collected in some of the profiled areas in order to measure their composition. The samples have been powdered and 0.5 g from each one has been dissolved in 250 ml of distilled water in accordance with the solubility of calcium sulphate in water. The solutions were shaken for 24 hours and then filtered. The residue left after filtering correspond to the non-soluble phases, which are made up of the lutitic matrix (including carbonates, quartz and other minor accompaining minerals). The residue was weighted in order to estimate the fraction of the in sulphate phases.

2.3 Results and discussion

In the Beuda quarry some different areas have been studied. The profiles A and B have been performed upon areas in which massive anhydrite was found and afterwards was buried under quarry waste materials. The profiles were spread above the infilling. The result of the inversion for Profile A (Figure 3A) display an upper part with relatively low electrical resistivity values (between 10 and 200 Ω.m), which corresponds to the quarry waste. Underlying these materials there is a homogeneous body with high resistivity value (up to 10^4 Ω.m), which has been interpreted as pure anhydrite (Lugo et al., 2008). In the case of Profile B, which was performed perpendicularly to Profile A, the inverted resistivity section (Figure 3B) displays a lateral electrical resistivity variation below the quarry waste layer. A well was drilled in the middle of profile B and high hardness was found at 6 meter depth, but no core was recovered. This hardness has been interpreted as anhydrite rock with certain quantity of matrix.

The profile C has been measured in other location where anhydrite had also stopped the exploitation of the quarry. The electrodes were inserted almost directly into the sulphate rocks and

both anhydrite and gypsum appeared in the ground surface. In the inverted resistivity section (Figure 3C) there is displayed a lateral variation of electrical resistivity ranging from 10^3 to 10^4 Ω.m. The larger resistivity values are limited with the outcropping of massive anhydrite, while the lower ones are related to the presence of gypsum, and the intermediate values correspond to the transition between the two pure phases.

Profile D has been performed in an abandoned quarry near to the village of Odena where anhydrite crops out. The inverted section (Figure 3D) shows electrical resistivities ranging from 10^3 to 10^4 Ω.m, similarly to the observations in the Beuda quarry. In the areas in which the value is larger, massive anhydrite is observed. Lower electrical resistivity than 500 Ω.m are related to lutitic sedimentary layers.

Profile E has been performed in an evaporitic basin with no outcrops. The inversion of the profile (Figure 3E) displays a shallow deposit with a low electrical resistivity value (50 Ω.m) which corresponds to the underlying materials. Below this layer there is a high resistivity body ranging from 1000 to more than 5000 Ω.m and with a more conductive structure in the central part (between 100 and 200 Ω.m). This structure represents a fault present in the area, and identified on the surface by geological evidence (Carrillo, 2009).

The profile F performed in Montes de Torrero area has been modified from Guinea et al. (2010b). In the inverted image (Figure 3F) the whole deposit shows a general trend of 30-50 Ω.m with some bodies slightly more resistive (up to 300 Ω.m at the most resistive points). Those bodies would represent a higher grade of the deposit (up to 60% in sulphates) in these zones, this grade changes are related to primary depositional processes and they are very common in these materials (Guinea et al., 2010a). In any case it is not possible to differentiate between anhydrite and gypsum layers because the electrical behavior of the deposit is dominated by the abundant matrix.

As general trend, sulphate rocks with high purity in anhydrite show an electrical resistivity value up to 10^4 Ω.m after the inversion (Lugo et al., 2008). This value is considered to be the reference

for pure anhydrite rocks because in some profiles in which some of the shallowest points have been measured almost directly above massive anhydrite rocks, show an apparent resistivity value larger than 5000 Ω.m. In these cases the apparent and the inverted resistivities are similar but a slightly lower for the apparent resistivity because the electrodes are inserted into a thin clay layer. When these rocks are mixed with gypsum forming pure sulphate rocks with both phases, which are the most common in the quarries, they display an intermediate value of resistivity ranging from 1500 to 5000 Ω.m depending on the quantity of each phase. As the distribution of the anhydrite in the gypsum deposits is very heterogeneous due to the rehydration processes, the tomography lines show heterogeneous bodies with different electrical resistivity values and transitional zones. Values close to 1000 Ω.m are related to the purest gypsum rocks or to pure anhydrite with a significant quantity of matrix rocks. When the matrix has a large volume fraction, it is not possible to differentiate is gypsum from anhydrite with ERT. In these cases, the rocks will display a resistivity below 100 Ω.m, which is significantly lower than the resistivity of sulphate-rich deposits. The low electrical resistivity of sulphate deposits with large matrix volume fraction was studied further by Guinea et al. (2010b) for the case of gypsum rocks (without anhydrite).

3. LABORATORY MEASUREMENTS

3.1 Methods

Many authors have measured the electrical conductivity of geological materials (Keller, 1966; Lockner and Byerlee, 1985; Guéguen and Palciauskas, 1994; Glover et al. 1996; Giao et al., 2003; Rusell and Barker, 2010; among others). Guinea et al (2010b) made eleven gypsum-clay pills in different proportions with a range from 0 to 100% of $CaSO_4 \cdot H_2O$ at intervals of 10% in composition and measured their electrical conductivity. Three sets of eleven anhydrite-lutite pills and three sets of gypsum-lutite pills have been made using the same methodology, parameters and resources. The compositional error of the pills is below 1%, because the weigh corresponding to the volume of each

fraction has been measured with a precision scale (mod. Sarorius B3100S) with a resolution of 0.01 g (the pills have a total weight of 13.5 g). The pills have a cylindrical shape with a radius of 2 cm and a width of approximately 0.50 cm. The aim of these measures is to define the importance of the matrix presence in calcium sulphate rocks.

The conductivity measurement was carried out in accordance with the UNE 21-303-33 regulation (1983) with an electrical circuit in which the samples act as electrical resistance (Figure 4). The electrical power source was a laboratory DC converter power supply with switchable voltage (0–32 V) and current (0-10 A). Changes in the amperage above 1A do not affect the essays so an output current of 2A has been selected. In order to measure the amperage of the electrical current after traversing the resistance (the sample), an analogical microammenter (Demestres, mod. 540) with a range of 0-100 μA with an accuracy of 1 μA or a nanoammeter (Monroe, mod. 285) with a range of ±200 nA and 0.1 nA resolution and an accuracy of 2% have been used. The potential difference is measured by a voltimeter (MY-67) with a resolution of 0.001 V connected to both sides of the pills. The electrodes used on the samples are made of stickers with metallic buttons as the ones used for electrocardiograms. The button has a conductive gel in the sticking side, forming a 0.75 cm-radius circled face (which will be considered the surface of the electrode). This gel is directly connected to the samples. The pills and the electrodes are situated above a paperboard insulator. The barreling effect is low because the distance between the electrodes is relatively small (approximately 0.50 cm). Due to the difference between the area of the electrodes and the area of the pills, there is a leak path for the electrical current (Roth, 1959). The measurements were made after the reading stabilizes (10 seconds after the power supply is switched on). Polarization causes errors after a certain time in the pills with large fractions of clay. The longest time measures are not considered representative for geophysical surveys because geoelectrical methods use a short current injection time. Each pill has been measured three times, making a total of 6 measurements for each volume fraction. Ohm's law can be applied to calculate the conductivity (σ) or resistivity (ρ) of the sample for a known current density (j) and field (E) (Eq. 1):

243 $$j = \sigma E = E/\rho$$

244 It is possible to measure the resistance (*R*) of the samples. As the thickness (*L*) of the sample
245 and the surface area of the electrode (*S*) are known, the electrical resistivity (ρ) can be calculated (Eq.
246 2):

247 $$R = \rho \, {}^{L}/_{S}$$

248 *3.2 Results and discussion*

249 The resistivity calculated for the gypsum-lutite and anhydrite-lutite pill sets is shown in Figure
250 5 (full measurements table is shown in Annex 1). The mean resistivity is indicated by symbols
251 together with an error bar representing the standard deviation. The measures performed on gypsum-
252 lutite pills showed a similar trend to the one presented by Guinea et al. (2010b). The pills ranging from
253 70 to 100% in gypsum fraction were more accurate in the present study because the current was
254 measured with a nanoammeter instead a microammeter. The pills ranging from 0 to 40% in gypsum
255 fraction displayed a slightly increasing trend of the electrical resistivity (with a mean value ranging
256 from 6 to 33 Ω.m). The 50 and 60% gypsum fraction pills displayed a transitional range of resistivity
257 (with mean values of 72 and 137 Ω.m respectively). Finally, the pills with a volume fraction of
258 gypsum ranging from 70 to 100% displayed a resistivity of >700 Ω.m. The trend showed by the
259 anhydrite pills is similar to the one showed by the gypsum pills for the case of pills with a sulphate
260 fraction from 0 to 50%. There are slight differences between them, but both sets are in the same range
261 of resistivities. The anhydrite-pills with a sulphate fraction of 60% or above are noticeably more
262 resistive than their equivalent in gypsum pills (ranging from 1012 to 7609 Ω.m in mean resistivity).

263 It is evident that the grades below 60% are dominated by the lutitic matrix and the sulphate
264 component affects the measurement negligibly. The sulphate volume fractions above 70% showed
265 high resistivity values in which the dominant component is the sulphate phase. Between the two
266 differentiated trends there is a transitional zone which represents the loose of the connectivity of the

matrix. As in the measures of gypsum pills by Guinea et al. (2010b), the pills with large quantity of clay component polarize with measuring time. The chargeability of clay has been widely described before (Takakura, 2006; Deucester and Kaufmann, 2009).

Percolation theory states that in a cluster with a component randomly distributed (meaning the lutitic matrix for this case) there is a percolation threshold which represent the minimal quantity of the component required in order to obtain a long-range connectivity (Stauffer and Aharony, 1985). This theory has been widely used to predict characteristics of rocks as the connection of their porosity or fractures (Karmakar et al., 2003; Wang et al., 2007). When the fraction of the component is below the percolation threshold, the cluster is not considered to be connected. In our system the percolation is controlled by conduction through matrix which is much more conductive than the sulphate phase. Anhydrite or gypsum components are dielectric (act as resistances) and they conduct little electrical current while the matrix fraction is above the percolation threshold. Below the percolation threshold, the electrical current finds no connected pathways in the matrix and passes through the sulphates. Hence, the relative proportion of gypsum and anhydrite phases when the presence of matrix is above 40%, do not affect the electrical resistivity value of the whole rock.

4. THEORETICAL CALCULATIONS

4.1 Methods

Physical properties of rocks are mainly functions of their microstructure (Guéguen and Palciauskas, 1994). Two important mathematical approaches are effective medium theory (EMT) and percolation theory. The EMT (Kirpatrick, 1973) approximation is quite good for rocks with quasi-uniform distributions where only a small degree of heterogeneity is observed, although they cannot describe correctly the phenomenon of clustering (Guéguen et al., 1997) when the heterogeneity is large. Moreover, the knowledge of the geometric distribution and connectivity of the minor phase is of great importance. Percolation theory describes the medium in terms of probabilities of the connectivity

but does not provide bulk physical properties. Here, we propose a method to determine the physical properties of composite materials that combines the EMT and the percolation theory. On one hand, the EMT is used to calculate the bounds of the physical properties depending on the amount of the matrix phase present. These limits correspond to the two extreme situations where t he matrix phase is totally interconnected or disconnected. On the other hand, the percolation theory is used to determine the probability of having a connected or interconnected matrix phase assuming that it is distributed in a single cube distribution.

The effective properties of composites, in particular electrical conductivity, have been studied analytically for a long time for a very simple cases (i.e., Maxwell (1881) used effective medium theory to derive the bulk conductivity of spheres dispersed in a continuous medium). The rocks can be considered as random materials of different property phases at various length scales. To compute the effective properties of such materials requires knowledge of the microstructure and require numerical computation. Garboczi (1999) wrote an algorithm and the consequent FORTRAN code to compute using both finite difference and finite element codes to calculate the electrical an elastic effective properties of materials with different phases from digital images.

In this paper the program ELECFEM2D.F from Garboczi (1999) has been used to compute the effective conductivity of gypsum-anhydrite rock samples. The method to calculate the electrical conductivity of these rocks is to analyze thin section images in which the amount of both anhydrite and gypsum proportion together with the one of the lutitic matrix is known. With this software it is possible to obtain a resistivity distribution model based on a microphotograph.

In order to perform the theoretical calculation of photographs with the program ELECFEM2D.F, the pictures must be converted from an image format file (e.g., JPG, JPEG, GIF, PNG) into an ASCII file. This has been carried out with a converter which creates numerical files from the pixels of the input image. Depending on the color range of these pixels, a numeric value, which is related to a user defined electrical resistivity value, is assigned. As the images used display lutite, gypsum and anhydrite phases; 10, 10^3 and 10^4 Ω.m electrical resistivity values have been selected

318 respectively. This selection will be discussed further in Section 4.2. The number of variables is user
319 defined and 2 variables (1 and 2) have been selected for photographs displaying 2 phases (any couple
320 of lutite-gypsum-anhydrite) and 3 variables (1, 2 and 3) when the 3 of them are present. Each image
321 was previously treated with an image processing program in order to homogenize the color ranges in
322 order to improve the detection of each phase.

323 Once the ASCII file is created, it can be used by the ELECFEM2D.F program. The program
324 divides the surface into 8400 (150×56) cells with an electrical resistivity value assigned to each one,
325 and calculates the current intensity remaining after crossing the system in the *x* or *y* direction. Both
326 directions and the arithmetic mean value have been calculated; the differences are related to the
327 anisotropic distribution of the phases. The selected potential gradient was set to 1 V/m.

328 *4.2 Mixing models for two and three phase systems*

329 Many mixing models have been published in order to predict the bulk conductivity of a porous
330 medium (Glover et al. 2000). In the case of sulphate rocks there is no porosity; hence, the resistivity
331 (or conductivity) of the bulk rock depends on the fraction (γ) and the electrical resistivity value (ρ) of
332 each component and on the connectivity and geometrical distribution of the matrix (which has the role
333 of a conducting fluid in a saturated porous medium). Different mixing models (Parallel, Perpendicular,
334 Random, Modified Archie's law and Hashin Shtrickman bounds) have been calculated for the case of
335 two-phase sulphate rocks (gypsum-lutite and anhydrite-lutite) with different proportions of sulphate
336 and matrix. The electrical resistivity values selected for gypsum and lutite phases have been 10^3 and
337 10 Ω.m, respectively (Guinea et al., 2010b). The electrical resistivity value selected for pure anhydrite
338 phase has been 10^4 Ω.m, in accordance with the maximum value measured in field examples and the
339 bibliography (Table 2).

340 Parallel and Perpendicular mixing models (Table 3A and B; Somerton, 1992; Guéguen and
341 Palciauskas, 1994) describe the conductivity of a layered distribution of phases with a constant
342 arbitrary thickness arranged axially or normally (in each case) to the current flow. The random model

(Table 3C; Warren and Price, 1961; Shankland and Waff, 1977) describes the bulk conductivity of a material with randomly distributed arbitrary volumes of the conductive phase. Glover (2000) described a mixing model (Table 3D) derived from Archie's law (Archie, 1942), considering the boundary conditions implied by geometrical constrains. To calculate this model, the cementation exponent *m* has to be defined for each phase. This variable depends on the connectedness of the phases and, as long as in the present case there is no information about this connectedness, it is considered that $m_1=m_2=1$. Hashin and Shtrikman (1963) defined the electrical resistivity value bounds (HS bounds) of a bulk rock from effective medium considerations. These bonds represent the theoretical maximum (upper bound; Table 3E) and minimum (lower bound; Table 3F) electrical resistivity value that any material formed of two different phases with a certain fraction can display.

The mentioned mixing models are displayed in the Figure 6 for both gypsum-lutite (Figure 6A) and anhydrite-lutite (Figure 6B) systems. The modified Archie's law model has the same trend that is calculated for the case of parallel model; this is because the cementation exponent *m* is considered 1 for every phase. Additionally to the theoretical trends of the mixing models, the resistivities calculated in the laboratory measurements are displayed. The pill samples with a fraction of sulphate phases of 50% or below show a similar trend to the one displayed by the HS^- model. This is also shown in the field data in the profiles in which the sulphate formations have a high quantity of matrix within. In the other hand, the resistivity of the pills with a sulphate fraction of 70% or above is closer to the perpendicular or HS^+ models. In the case of the anhydrite pills with high sulphate fraction, they fit better to the random model; but this can be related to the fact that the anhydrite pills are slightly watered during their elaboration. The field data obtained in anhydrite rocks also indicate that the observed resistivity ranges fit better to the perpendicular or HS^+ models. The values obtained for the pills with 60% in sulphate fraction are transitional, which represents the percolation threshold. Theoretically the percolation threshold occurs in a single phase fraction but in the case of real rocks transitional values are displayed in this range of composition.

From the trends observed for two-phase systems, it can be considered as approximation that the HS bounds define the resistivity of gypsum and anhydrite rocks depending on the quantity of

matrix present. When the matrix is percolating (sulphate fraction of 50% or below), the resistivity of the sulphate rocks is bounded to the HS- model. In the case of non percolating matrix (sulphate fraction of 70% or above), the resistivity is bounded to the HS^+ model. A general form of the bounds for n-phases was given by Berriman (1995). With his formula it is possible to construct a ternary graphic for 3-phased rocks (Ledo and Jones, 2005). The gypsum-Anhydrite-Lutite (GAL) system has been calculated for both upper (Table 3G) and lower (Table 3H) HS bounds. In the case of lower bound (Figure 7A), the system is clearly dominated by the lutitic component; the isoresistivity lines are parallel between them showing no appreciable variation in the gypsum-anhydrite axis but when the lutite fraction is less than 10%. The values of resistivity are very low in general, showing less than 100 Ω.m for a sulphate fraction of 70%. The upper bound (Figure 7B) displays a very different trend dominated by the anhydrite fraction, but in this case the 3 components affect the bulk resistivity value of the rock. The electrical resistivity values are much larger than in the case of lower bound achieving 1000 Ω.m with only 40% of anhydrite. As it has been previously shown, the electrical behavior of the rocks is the one of lower HS bound when the quantity of sulphate is of 50% or below and the one of upper bound when is of 70% or above. Thus it is expected that the real distribution of the electrical resistivity for the GAL system should be a combination between the upper and lower HS bounds (Figure 7C).

4.3 Results and discussion

In order to check the accurateness of this GAL diagram, the theoretical electrical resistivity value of real thin section rock photographs (Figure 8) has been calculated with ELECFEM2D program. Lutitic matrix display brownish coloring while both anhydrite and gypsum have are transparent underplane polarized light; having anhydrite higher relief than gypsum (its bounds are well marked with dark lines). With crossed polarized light, gypsum and anhydrite can be easily differentiated because of the different coloring of the anhydrite (pink, green, blue, …) in contrast with the gray colors of the gypsum crystals. The standard electrical resistivity values selected for the gypsum, anhydrite and lutitic matrix phases have been 10^3, 10^4 and 10 Ω.m respectively, as has been assigned before. The electrical resistivity of the bulk sections has been measured in both *x* and *y*

directions; when the distribution of the components is homogeneous these values would be considered similar. For each thin section the fractions of the components are calculated by the program so it is possible to obtain the electrical resistivity value corresponding to these fractions calculated with different mixing models (Table 4).

The results show that the mean of the calculated electrical resistivity values in *x* and *y* directions are in general close to HS^+ bound when the fraction of sulphate is 70% or higher (Figure 8, thin sections A, D, E, F, G and H; Table 4) and to the HS^- bound when the fraction of matrix is abundant (Figure 8, B and I; Table 4). There is a good match between the corresponding position of each sample in the figure 7C, according to their components percentages, and the calculated resistivity values. In the case of thin sections C and J there is abundant matrix (58 and 52% respectively); nevertheless, the calculated resistivity values are slightly larger than that expected for such mixture. This is due to that the phases are not scattered and randomly distributed within the samples but forming compact and pure areas. This represents large heterogeneities which change the percolating behavior (we have considered it only for regular distributions of the phases as in the case of the pills) of the bulk rock and makes the transition zone larger. In any case the values are always much closer to the lower bound that to the upper one. The parallel/Modified Archie's law and perpendicular (serie) models does not fit well to the calculated resistivities. The random model fits well in many cases but in samples with large fraction of anhydrite, calculated resistivity is too high (especially in C thin section).

At larger scale (as in the ERT profiles) the rocks are in general more homogeneous and should fit to the HS lower bound for compositions of 0-60% in lutitic matrix. The microscopic anisotropies do not affect to the electrical conductivity of the bulk deposit if we increase the scale. In any case, it is possible to observe cases of heterogeneities at metric scale. When these heterogeneities are large, they can be considered as different rocks (for example a gypsum-rich lutite body within a larger pure gypsum host-rock). In any case, heterogeneities below the detection limit of the method will be considered as a single rock. Another possible case is a layered deposit in which every layer has different purity in the sulphate phase. If the difference among grades is low, which is the most

common case, the whole sequence can be considered as a single member with a mean grade. Rarely sulphate deposits have great variations of grade from layer to layer forming a heterogeneous sequence. Sudden variations in the grade exist, but are normally associated with the limit of a sequence or a stable change in the depositional conditions. In the case of having layering between almost pure matrix and highly pure sulphates, the transitional values of resistivity will increase their range as happens in the case of the microphotographs.

5 GEOELECTRICAL CLASSIFICATION OF CALCIUM SULPHATE ROCKS

With the GAL diagram obtained combining both HS^+ and HS^- boundaries for a gypsum anhydrite-lutite system (Figure 7C) a geoelectrical classification has been elaborated differentiating 6 calcium sulphate rock types (Figure 9). When the lutitic matrix is connected at long range (in the case of sulphate fraction of 50% or below) the system is matrix dominant and therefore there is no possibility of differentiating between gypsum and anhydrite components; these rocks are classified as Lutites and Gypsum/Anhydrite rich Lutites. The electrical resistivity of this groups range from 10 to 100 Ω.m. When the sulphate grade is of 70% or above, the rock will be considered as pure Gypsum when it ranges from 700 to 1000 Ω.m as was stated by Guinea et al. (2010b) for the case of gypsum-lutite systems. If the sulphate mineral is mainly anhydrite (more than 90%) the rock is considered pure Anhydrite and its electrical resistivity value range from 2500 to 10^4 Ω.m depending on the rock grade. In the case of presence of both gypsum and anhydrite sulphate phases, the rock is considered Gypsum with Anhydrite (1000 to 2000 Ω.m) or Anhydrite with Gypsum (2000 to 5000 Ω.m). The values of pure Anhydrite and Anhydrite with Gypsum overlap; in this case it is possible to bond the electrical value to Pure Anhydrite rocks when there is no evidence of rehydration and to the Anhydrite with Gypsum otherwise. Between Lutites and Gypsum/Anhydrite rich Lutites and the sulphate pure rocks there is a transitional area displaying transitional values from 100 to 700/2500 Ω.m (depending of the sulphate composition). The lower boundary of Transitional Gypsum/Anhydrite rocks has been selected as 55% in sulphate fraction instead of 60% because the measures in pills have shown that the 60%

values display an electrical resistivity increasing trend; the upper boundary is 70% in gypsum fraction. This transitional area is displayed with a resistivity-trend calculated by interpolation between lower and upper HS bounds, but the resistivity in the transition zone is uncertain and therefore the displayed trend is only a reference.

For the microscopic scale, it has been shown that the transitional range is wider (including rocks between 55 and 70% in sulphate fraction, depending of the anisotropy). For the cases of sulphate fractions of 55% or below or higher than 70%, the values obtained are similar to the corresponding HS bound. At larger scale, the ERT lines have shown relationships between composition and resistivity values similar to the ones displayed in the classification of the Figure 9; that is, higher than 5000 Ω.m when the dominant phase is the anhydrite, 1500 to 5000 Ω.m for different proportions of gypsum and anhydrite (with presence of little lutite) and close to 1000 Ω.m when the gypsum is the dominant phase. For deposits with large amount of lutites, the obtained value has been <60 Ω.m in all cases.

6. CONCLUSIONS

The electrical properties of calcium sulphate rocks have been widely studied at different scales with microphotographs, synthetic pills and geological deposits. Laboratory tests in pills have shown that the matrix of calcium sulphate rocks may be affected by the percolation phenomena and therefore, when the sulphate fraction in a rock is of 55% or below, the matrix controls the resistivity of the bulk rock. When the sulphate fraction is of 70% or above, the sulphate minerals control the electrical resistivity of the bulk rock.

The electrical resistivity value of anhydrite rocks range from 10 to 10^4 Ω.m, being larger in the purest anhydrite rocks. This value is found in the field examples where the anhydrite appears in massive form. The values observed in rocks with both gypsum and anhydrite (with minor matrix) have ranged between 1500 and 5000 Ω.m depending on the quantity of each other. Large quantity of matrix

in sulphate rocks have shown low electrical resistivity values been unable to differentiate between gypsum and anhydrite.

When the matrix of the calcium sulphate rocks is above the percolation threshold (i.e., more than 45%), the electrical resistivity value fits the value calculated with the Hashin-Shtrikman lower bound (HS^-), and when is embedded in the sulphate phase (i.e., 30% of matrix or less) the resistivity follows the Hashin-Shtrikman upper bound (HS^+). If there are large heterogeneities in the distribution of the phases, the resistivities of rocks with a matrix quantity ranging from 30 to 45% can display transitional values (more than 100 Ω.m, without reaching values of the purest sulphate rocks). Therefore, it is possible to calculate any combination of these 3 components and the geoelectrical classification has been elaborated for calcium sulphate rocks. With this classification is possible to determine the purity of the sulphates and the presence of anhydrite in gypsum rocks, which is useful for the characterization of the deposit.

ACKNOLEDGEMENTS

The present work is a part of a PhD thesis supported by the "Programa General d'Intensificació de la Recerca" (Generalitat de Catalunya-UB) and the Spanish Government Projects CGL2009-11096, CGL2009-07025, CGL2010-18260 and CGL2009-07604. We want to appreciate the support and facilities of Drs. Albert Casas, Esperança Tauler and Manel Labrador (Universitat de Barcelona, UB) and Dr. Ricard Bosch (Universitat Politècnica de Barcelona, UPC). We also want to thank to Grupo Uralita Corporation, especially to Ms. Mayte Martín, for letting us work in the quarry of Beuda and their support.

REFERENCES:

Asfahani, J., Mohamad, R., 2002. Geo-electrical investigation for sulphur prospecting in Teshreen Structure in Northeast Syria. Exploration and Mining Geology, 11, 49-59.

Archie, G.E., 1942. The electrical resistivity log as an aid in determining some reservoir characteristics. Transactions of the American Institute of Mining, Metallurgical, and Petroleum Engineers, 146, 54-62.

Ayora, C., García-Veigas, J., Pueyo, J.J., 1994. The chemical and hydrological evolution of an ancient potash-forming evaporite basin as constrained by mineral sequence, fluid inclusion composition and numerical simulation. Geochimica et Cosmochimica Acta, 58, 3379-3394.

Berriman, J.G., 1995. Mixture theories for rock properties. In: T.J. Ares Ed., Rock Physics and Phase Relations: A Handbook of Physical Constants. American Geophysical Union, Washington, 236pp.

Bustillo, M., Calvo, J.P., Fueyo, L., 2001. Rocas Industriales: Tipología, aplicaciones en la construcción y empresas del sector. Rocas y Minerales (ed.). 410pp.

Carrillo, E., 2009. Unidades evaporíticas eocenas de la Zona Surpirenaica Oriental (Área de La Garrotxa). Geogaceta, 47, 73-76.

Chouteau, M., Phillips, G., Prugger, A., 1997. Mapping and monitoring softrock mining. In: Proceedings of Exploration 97: Fourth Decennial International Conference of Mineral Exploration, A.G. Gubins Ed., 927-940.

Deucester, J.& Kaufmann, O., 2009. Correlation between inverted chargeabilities and organic compounds concentrations in soils-A field experiment. 15th Near Surface meeting, Dublin, Ireland, Expanded Abstracts, C19.

Furman, A., Ferré, P.A., Warrik, A.W., 2003. A Sensitivity Analysis of Electrical Resistivity Tomography Array Types Using Analytical Element Modeling. Vadose Zone Journal, 2, 416-423.

520 Garboczi, E.J., 1999. Finite element and finite difference programs for computing the linear
521 electric and elastic properties of digital images of random materials. NIST Internal Report 6269. Also
522 available at http://ciks.cbt.nist.gov/garbocz/

523 Giao, P.H., Chung, S.G., Kym, D.Y., Tanaka, H., 2003. Electric imaging and laboratory
524 resistivity testing for geotechnical investigation of Pusan clay deposits. Journal of Applied
525 Geophysics, 52, 157-175.

526 Glover, P.W.J., Gomez, J.B., Meredith, P.G., Boon, S.A., Sammonds, P.R., Murrell, S.A.F.,
527 1996. Modelling the Stress/Strain Behaviour of Saturated Rocks Undergoing Triaxial Deformation
528 using Complex Electrical Conductivity Measurements, In Integrated Experimental Measurements and
529 Theoretical Modelling of Rock Transport Properties. Surveys in Geophysics, 17, 307-330.

530 Glover, P.W.J., Hole, M.J., Pous, J., 2000. A modified Archie's law for two conducting
531 phases. Earth and Planetary Science Letters, 180, 369-383.

532 Guéguen, Y., Chelidze, T., Le Ravalec, M., 1997. Microstructures, percolation thresholds, and
533 rock physical properties. Tectonophysics, 279, 23-35.

534 Guéguen, Y., Palciauskas, V., 1994. Introduction to the physics of rocks. Princenton
535 University Press, Princenton, NJ, 294pp.

536 Guinea, A., Playà, E., Rivero, L., Salvany, J.M., Himi, M., 2009. Geoelectrical imaging
537 supporting glauberite deposits evaluation in the Montes de Torrero area (Zaragoza). Geogaceta, 47,
538 145-148.

539 Guinea, A., Playà, E., Rivero, L., Himi, M., 2010a. Electrical Resistivity Tomography and
540 Induced Polarization techniques applied to the identification of gypsum rocks. Near Surface
541 Geophysics, 8, 249-257.

Guinea, A., Playà, E., Rivero, L., Himi, M., Bosch, R., 2010b. Geoelectrical Classification of Gypsum Rocks. Surveys in Geophysics, 31 (6), 557-580.

Hashin, Z., Shtrikman, S., 1963. A variational approach to the theory of the elastic behavior of multiphase materials. Journal of the Mechanics and Physics of Solids, 11, 12-140.

Holliday, D.W., 1970. The petrology of secondary gypsum rocks: a review. Journal of Sedimentary Petrology, 40, 734-744.

Inglés, M., Manote, M.R., Ortí, F., Pey, J., Playà, E., Rosell, L., Yeguas, J., 2009. Geochemical methods in alabaster provenance: an application example. IX ASMOSIA: Interdisciplinary Studies on Ancient Stone meeting, Tarragona, Spain, Abstracts 125.

Jakosky, J.J., 1950. Exploration geophysics. Trija Publishing Co., Los Angeles, 1195pp.

Karmakar, R., Manna, S.S., Dutta, T., 2003. A geometrical model of diagenesis using percolation theory. Physica A, 318, 113-120.

Keller, G.V., 1966. Electrical properties of rocks and minerals. In: Clark S.P. (Ed.), Handbook of physical constants. The Geological Society of America, 587pp.

Kirkpatrick, S., 1973. Percolation and conduction. Reviews of Modern Physics, 45, 574-588.

Klein, C., Hurlburt, C.S., 1998. Manual de mineralogía de Dana. Reverté, 438pp.

Ledo, J., Jones, A.G., 2005. Upper mantle temperature determined from combining mineral composition, electrical conductivity laboratory studies and magnetotelluric field observations: Application to the intermontane belt, Northern Canadian Cordillera. Earth and Planetary Science Letters, 236, 258-268.

Loke, M.H., Baker, R.H., 1996. Rapid least-squares inversion of apparent resistivity pseudosections by a quasi-Newton method. Geophysical Prospecting, 44, 131-152.

564 Lockner, D.A., Byerlee, J.D., 1985. Complex resistivity measurements in confined rock.
565 Journal of Geophysical Research, 90, 7837-7847.

566 Lugo, E., Playà, E., Rivero, L., 2008. Aplicación de la tomografía eléctrica a la prospección de
567 formaciones evaporíticas. Geogaceta, 44, 223-226.

568 Ma, Y., Wang, H., Xu, L.A., Jiang, C., 1997. Simulation study of the electrode array used in
569 an ERT system. Chemical Engineering Science, 52, 2197-2203.

570 Maxwell, J., 1881. A Treatise on Electricity and Magnetism. Clarendon, Oxford, 2nd edition,
571 540pp.

572 Ortí, F., 2000. Unidades glauberíticas del Terciario ibérico: nuevas aportaciones. Revista de la
573 sociedad geológica de España, 13, 227-249.

574 Ortí, F., Rosell, L., Playà, E., García-Veigas, J., 2010. Large gypsum nodules in the Tertiary
575 evaporites of Spain: distribution and paleogeographic significance. Geological Quarterly, 54 (4), 411-
576 422.

577 Parkhomenko, E.J., 1967. Electrical properties of rocks. Plenum Press, New York, 314pp.

578 Rider, M.H., 1986. The Geological interpretation of well logs. Blackie Halsted Press, 175pp.

579 Robinson, E.S., Çoruh, C., 1988. Basic Exploration Geophysics. Jonh Wiley and sons, 562pp.

580 Rosell, L., Pueyo, J.J., 1997. Second marine evaporitic phase in the South Pyrenean Foredeep:
581 the priabonian potash basin (Later Eocene: Autochthonous-Allochthonous Zone). In: Busson, G.,
582 Schreiber, Ch. Eds. Sedimentary deposition in rift and foreland basins in France and Spain. Columbia
583 University Press, New York, 358–387.

584 Roth, A., 1959. Hochspannungstechnik. Springer, 756pp.

585 Rusell, E.J.F., Barker, R.D., 2010. Electrical properties of clay in relation to moisture loss.
586 Near Surface Geophysics, 8, 173-180.

587 Salvany, J.M., 2009. Geología del yacimiento glauberítico de Montes de Torrero (Zaragoza).
588 Prensas Universitarias de Zaragoza, 72pp.

589 Shankland, T.J., Waff, H.S., 1977. Partial melting and electrical conductivity anomalies in the
590 upper mantle. Journal of Geophysical Research, 82, 5409-5417.

591 Shearman, D.J., 1985. Syndepositional and late diagenetic alteration of primary gypsum to
592 anhydrite. In: Schreiber, B.C., (Ed.), Sixth International Symposium on Salt, vol. 1, Salt Institute, 41-
593 55.

594 Somerton, W.H., 1992. Thermal properties and temperature-related behavior of rock/fluid
595 systems. Elsevier, Amsterdam, 257pp.

596 Stauffer, D., Aharony, A., 1985. Introduction to percolation theory. Taylor and Francis (Eds.),
597 181pp.

598 Szalai, S., Szarka, L., 2008. On the classification of surface geoelectric arrays. Geophysical
599 Prospecting, 56, 159-175.

600 Takakura, S., Nakada, K., 2006. IP measurements on tunnel walls of a sericite deposit – A
601 contact method of nonpolarizable electrodes on a base rock and detection of clay minerals by
602 normalised chargeability. Geophysical Exploration, 59, 363–370.

603 UNE 21-303-83, norma española, 1983. Métodos para la medida de la resistividad transversal
604 y superficial de los materiales aislantes eléctricos sólidos. Instituto Español de Normalización.

605 Wang, K.W., Sun, J.M., Guan, J.T., Zhu, D.W., 2007. A percolation study of electrical
606 properties of reservoir rocks. Physica A, 380, 19–26.

607 Warren, J.E., Price, A.C., 1961. Flow in heterogeneous porous media. Society of Petroleum
608 Engineers Journal, 1, 153-169.

609 Warren, J.K., 2006. Evaporites: sediments, resources and hydrocarbons. Springer, 1035pp.
610

TABLE CAPTIONS

Table 1: Geoelectrical classification of gypsum rocks (modified after Guinea et al. 2010b).

Table 2: Electrical resistivity values for anhydrite rocks in the literature.

Table 3: Summary of the equations of the mixing models used in the present study (modified from Glover et al. 2000).

Table 4: Results of the theoretical calculations of electrical resistivity of the thin section photographs with ELECFEM2D software. Parallel, Serie, Random, Archie's modified law and Lower (HS^-) and upper (HS^+) Hashin-Shtrikman bounds have been calculated, only considering the proportion of each phase. The calculated resistivity for each sample in both x^- and y^- directions is listed in the right column. The corresponding images of the thin sections A to J are displayed in Figure 8.

FIGURE CAPTIONS

Figure 1: Photographs of the areas studied with ERT, A to C are taken in the Beuda quarry while D is taken in the area of Odena and E in the Zaragoza formation. A) pure gypsum-anhydrite boundary with a interdigitation between them; B) sulphate layers showing less gypsum fraction than in other areas; C) anhydrite blocks filled with gypsum veins and embedded in a gypsum matrix; D) massive anhydrite body; E) impure sulphate layers in Montes de Torrero area.

Figure 2: Distribution of evaporite formations in the Tertiary basins northeastern Spain indicating the location of the nine studied ERT profiles with black dots (modified from Ortí et al., 2010).

Figure 3: Inverted electrical resistivity tomography data for the different areas studied (the locations of the profiles are shown in figure 2). Profile F modified from Guinea et al. (2010b).

Figure 4: Electrical circuit to measure the electrical resistivity of the samples. It consists of a switchable laboratory power-supply (EA-PS 3032-10B), two electrodes, a voltimeter (MY-67) and a

micro or nanoammeter depending on the samples (Demestres, mod. 540; and Monroe, mod. 285 respectively).

Figure 5: Semi-logarithmic plots representing the results of the measurements of gypsum-lutite (A) and anhydrite-lutite (B) pills. The symbols represent the mean of the calculated resistivities for each sulphate fraction (using 2 pills and 3 different measurements on both for each fraction) and the error bar represents the standard deviation. The error on the X axis is not showed because is below 1%.

Figure 6: Different mixing models calculated for the case of gypsum-lutite (A) and anhydrite-lutite rocks (B). The resistivity ranges obtained in the laboratory essays (Figure 5) are superimposed for both cases.

Figure 7: Ternary plots showing Hashin-Shtrikman bounds for gypsum-anhydrite-lutite (GAL) system. A) lower HS bound; B) upper HS bound; C) combined diagram considering the percolation phenomena.

Figure 8: Microphotographs of thin sections of calcium sulphate rocks; D, E, H and I are taken with cross polarized light and the rest with plane polarized light. The different phases are indicated with numbers 1 (gypsum), 2 (anhydrite) and 3 (lutite/carbonate).

Figure 9: Geoelectrical classification of calcium sulphate rocks, depending on their gypsum-anhydrite-lutite fraction. The resistivity values are shown in the background (Figure 7C).

ANNEX

Annex 1: Results of the laboratory measurements on synthetic pills made by mixing powdered pure anhydrite or gypsum with clay. G samples correspond to gypsum-lutite pills, while A samples correspond to anhydrite-lutite pills. Samples with a sulphate fraction of 70% or above have been measured with a nanoammeter and the rest with a microammeter. The mean resistivity for each fraction and the standard deviation is showed in Figure 5.

Table 01

Click here to download high resolution image

	Purity in Gypsum (%)	Resistivity (ohm.m)
Lutites and Gypsum rich Lutites	0-55	10-100
Transitional Gypsum	55-75	100-700
Pure Gypsum	75-100	700-1000

Table 02

Click here to download high resolution image

REFERENCE	RESISTIVITY (ohm.m)	AUTHOR'S COMMENTS
Lugo et al. (2008)	1000-11500	The bodies displaying the lowest values are related to the presence of gypsum from the hydration of anhydrite while the highest ones are related to pure anhydrite.
Asfahani and Mohammad (2002)	94-1200	The values are measured by vertical electrical soundings in a gypsum and anhydrite formation.
Choteau et al. (1997)	1000	Anhydrite appears in an halite-karnalite-tachyhydrite sequence.
Robinson and Çoruh (1988)	10^{9}-10^{10}	Anhydrite appears in a summary of different mineral resistivity values
Rider (1986)	10^{4}-10^{10}	Obtained from wireline logs of different sources.
Parkhomenko (1967)	1.0 -10^{9}	Listed in a summary of different mineral and rock resistivities
Jakosky (1950)	1.0 -10^{3} / 1.0-10^{5}	Low and High resistivity ranges obtained from laboratory measurements

Table 03

Name	Conducting phases	Equation
a) Parallel model	1+	$\sigma_{\text{eff}} = \sum_{i=1}^{N} \chi_i \sigma_i$
b) Perpendicular model	1+	$\frac{1}{\sigma_{\text{eff}}} = \sum_{i=1}^{N} \frac{\chi_i}{\sigma_i}$
c) Random model	1+	$\sigma_{\text{eff}} \prod_{i=1}^{N} \sigma_i^{\chi_i}$
d) Modified Archie's law	1-2	$\sigma_{\text{eff}} = \sigma_1(1-\chi_2)^p + \sigma_2 \chi_2^m$ where $p = \frac{\log(1-\chi_2^m)}{\log(1-\chi_2)}$
e) Hashin–Shtrikman upper bound	2	$\sigma_{\text{eff}+} = \sigma_2\left(1 - \frac{3(1-\chi_2)(\sigma_2-\sigma_1)}{3\sigma_2 - \chi_2(\sigma_2-\sigma_1)}\right)$
f) Hashin–Shtrikman lower bound	2	$\sigma_{\text{eff}-} = \sigma_1\left(1 + \frac{3\chi_2(\sigma_2-\sigma_1)}{3\sigma_1 + (1-\chi_2)(\sigma_2-\sigma_1)}\right)$
g) Hashin–Shtrikman upper bound	3	$\sigma_{\text{eff}+} = \frac{1}{\left(\frac{\chi_1}{\sigma_1+2\sigma_2}\right) + \left(\frac{\chi_2}{3\sigma_2}\right) + \left(\frac{\chi_3}{\sigma_3+2\sigma_2}\right)} - \sigma_2$
h) Hashin–Shtrikman lower bound	3	$\sigma_{\text{eff}-} = \frac{1}{\left(\frac{\chi_1}{\sigma_1+2\sigma_3}\right) + \left(\frac{\chi_2}{\sigma_2+2\sigma_3}\right) + \left(\frac{\chi_3}{3\sigma_3}\right)} - 2\sigma_3$

Table 04

Click here to download high resolution image

	COMPOSITION (%)			MIXING MODEL (Ω.m)					CALCULATED (Ω.m)	
Thin section	Gy	Anh	Lut	Parallel	Series	Random	HS-	HS+	X	Y
A	95	0	5	168	951	794	365	928	862	844
B	17	0	83	12	178	22	16	129	16	16
C	0	42	58	17	4206	2630	32	1091	214	126
D	0	83	17	59	8302	3090	154	4504	3087	3157
E	29	71	0	2770	7390	5129	4417	6684	5070	6024
F	68	32	0	1404	3880	2089	1947	3230	1622	2265
G	26	51	23	43	5361	1122	105	2105	1102	2474
H	53	34	13	74	3931	1202	185	1708	1129	1940
I	35	6	59	17	956	76	30	408	33	82
J	38	10	52	19	1385	115	36	540	65	210

Annex 01

Click here to download Table: Annex 01.xlsx

Sample	Sulphate fraction (%)	Thickness (cm)	Voltage 1 (mV)	Voltage 2 (mV)	Voltage 3 (mV)	Current 1 (µA)	Current 2 (µA)	Current 3 (µA)	Resistivity 1 (Ω.m)	Resistivity 2 (Ω.m)	Resistivity 3 (Ω.m)
G1	0	0.49	12	11	13	90	90	95	5	4	5
G1'	0	0.49	15	23	11	74	96	78	7	9	5
G2	10	0.49	22	14	12	70	64	28	11	8	15
G2'	10	0.49	14	12	23	60	56	73	8	8	11
G3	20	0.50	11	15	14	28	35	37	13	15	13
G3'	20	0.50	15	12	12	42	40	14	12	11	30
G4	30	0.49	16	31	21	28	48	74	20	23	10
G4'	30	0.50	18	14	12	36	24	49	18	21	9
G5	40	0.52	33	30	35	37	37	78	30	28	16
G5'	40	0.50	34	42	45	21	50	38	57	30	40
G6	50	0.51	41	19	36	20	23	39	71	29	32
G6'	50	0.50	43	40	42	12	14	21	126	101	71
G7	60	0.52	26	30	29	10	12	8	88	85	123
G7'	60	0.51	32	41	21	6	9	4	185	158	182
G8	70	0.51	3	2	3	0.120	0.096	0.144	866	722	722
G8'	70	0.50	2	3	4	0.070	0.132	0.139	1009	803	1017
G9	80	0.52	3	3	2	0.092	0.067	0.095	1108	1522	715
G9'	80	0.52	4	3	3	0.126	0.132	0.067	1078	772	1522
G10	90	0.51	3	2	1	0.070	0.050	0.036	1484	1386	962
G10'	90	0.51	2	4	2	0.082	0.088	0.040	845	1575	1732
G11	100	0.52	1	1	1	0.013	0.016	0.012	2613	2124	2832
G11'	100	0.53	2	1	1	0.040	0.022	0.030	1667	1515	1111
A1	0	0.49	16	15	14	97	93	94	6	6	5
A1'	0	0.48	13	17	11	89	92	88	5	7	5
A2	10	0.49	15	18	19	55	60	57	10	11	12
A2'	10	0.50	18	22	12	62	67	67	10	12	6
A3	20	0.50	17	26	18	40	43	37	15	21	17
A3'	20	0.50	20	19	22	42	44	45	17	15	17
A4	30	0.50	18	22	25	33	40	35	20	20	26
A4'	30	0.51	23	24	32	26	28	26	31	30	43
A5	40	0.50	36	23	43	33	24	58	37	13	25
A5'	40	0.50	32	32	56	66	62	71	17	18	28
A6	50	0.52	29	44	44	41	42	50	25	36	30
A6'	50	0.50	35	37	50	32	33	30	39	40	59
A7	60	0.52	43	55	39	2	3	2	731	623	663
A7'	60	0.53	31	43	43	1	1	1	1074	1490	1490
A8	70	0.51	2	1	1	0.035	0.028	0.022	1980	1237	1575
A8'	70	0.52	1	2	2	0.023	0.026	0.033	1537	2718	2142
A9	80	0.53	2	1	2	0.021	0.013	0.021	3236	2614	3236
A9'	80	0.52	2	2	1	0.033	0.037	0.019	2059	1837	1788
A10	90	0.52	1	1	1	0.007	0.009	0.010	4950	3850	3465
A10'	90	0.53	1	1	1	0.009	0.004	0.007	3850	8662	4950
A11	100	0.52	1	1	1	0.004	0.005	0.008	8495	6796	4248
A11'	100	0.52	1	1	1	0.005	0.003	0.004	6668	11113	8335

Figure 01
Click here to download high resolution image

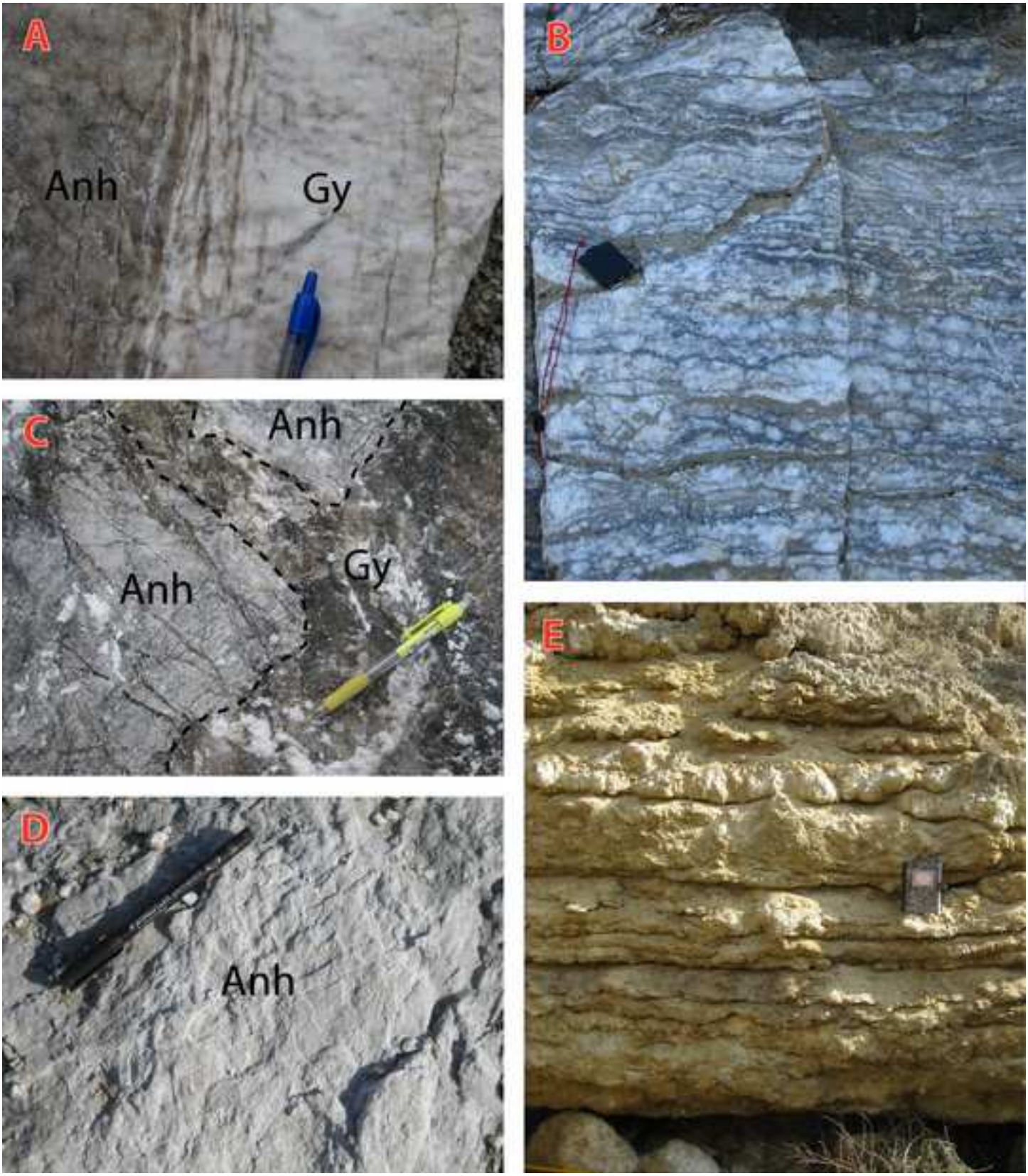

Figure 02

Click here to download high resolution image

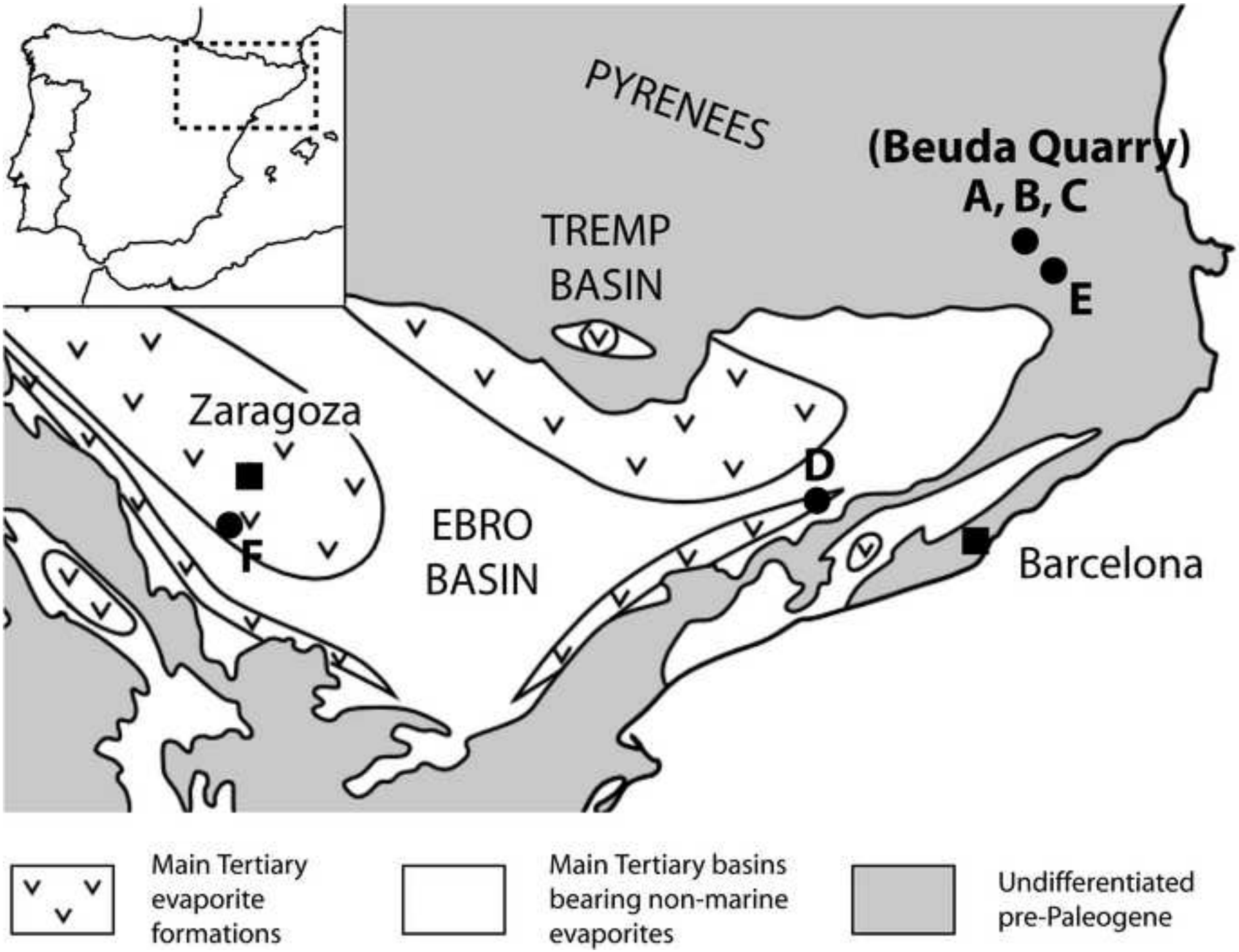

Figure 03

Click here to download high resolution image

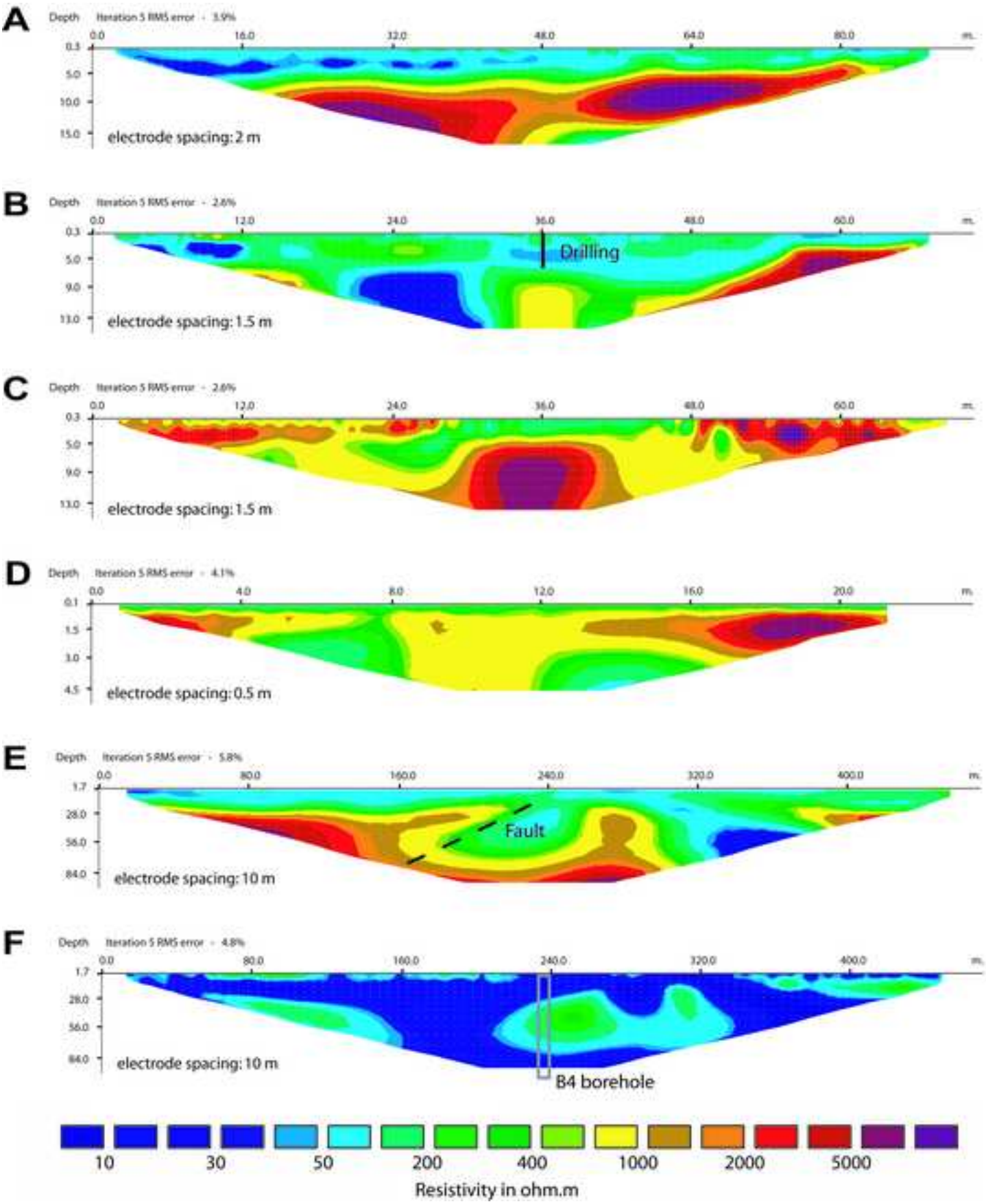

Figure 04

Click here to download high resolution image

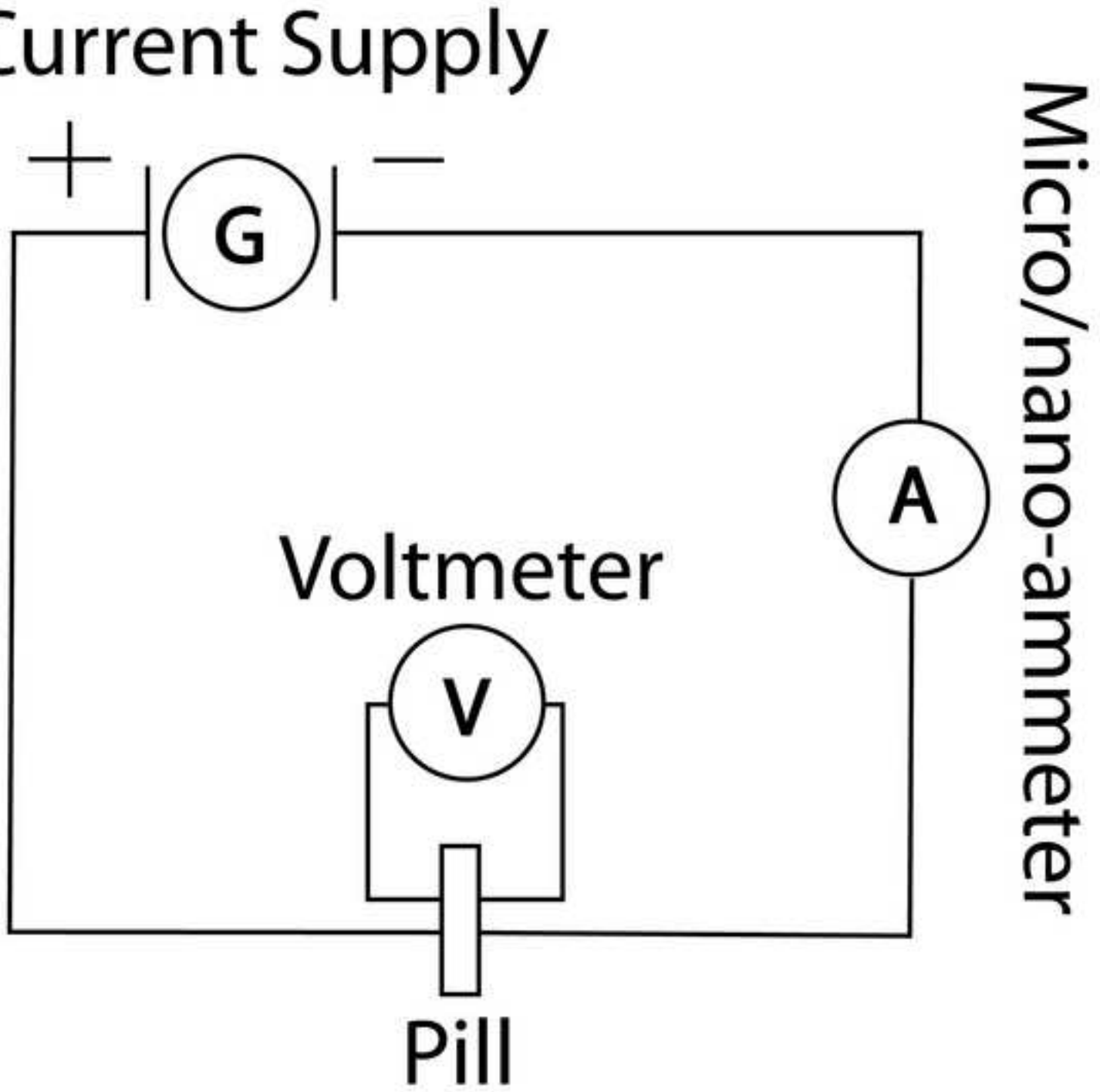

Figure 05
Click here to download high resolution image

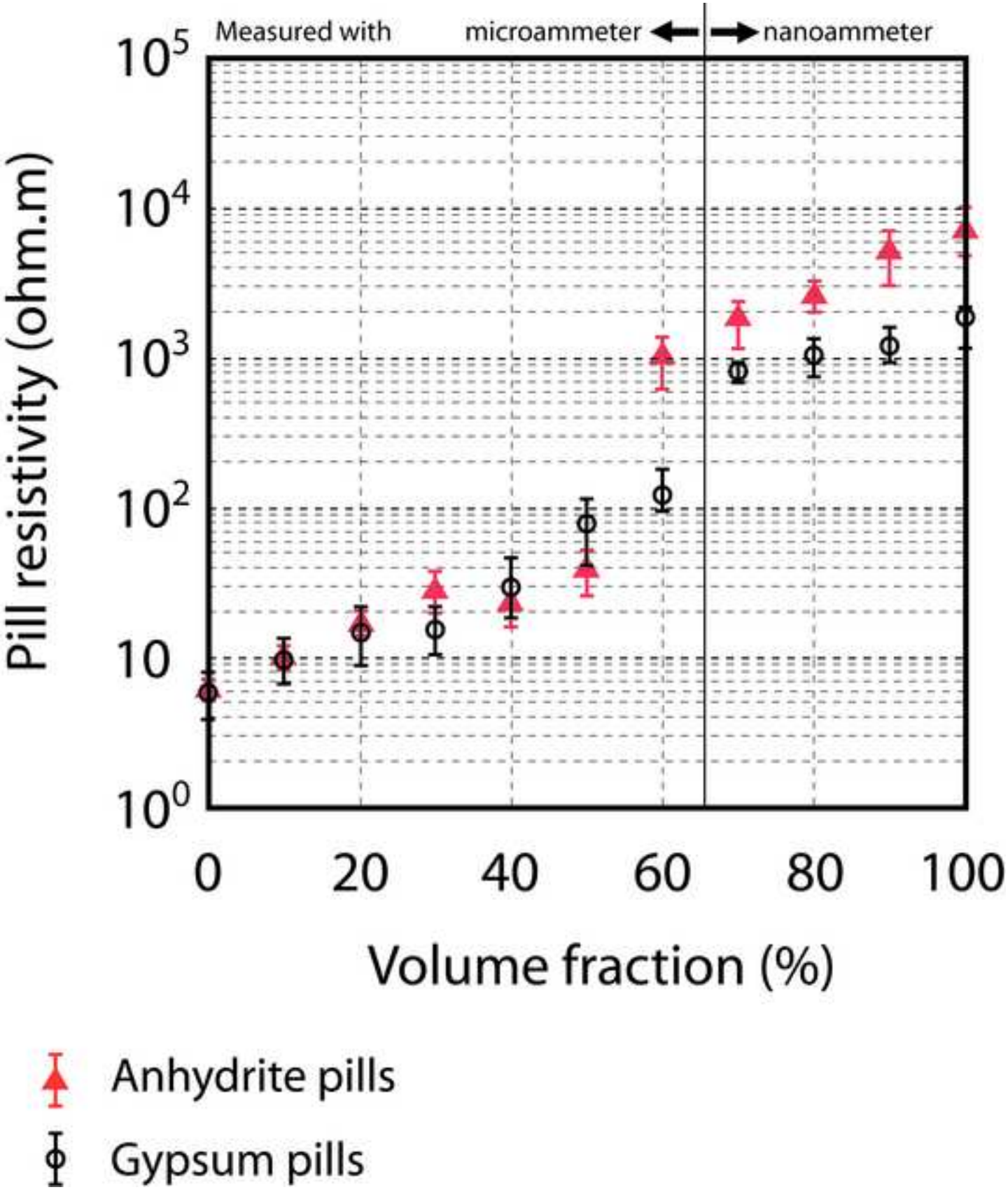

Figure 06

Click here to download high resolution image

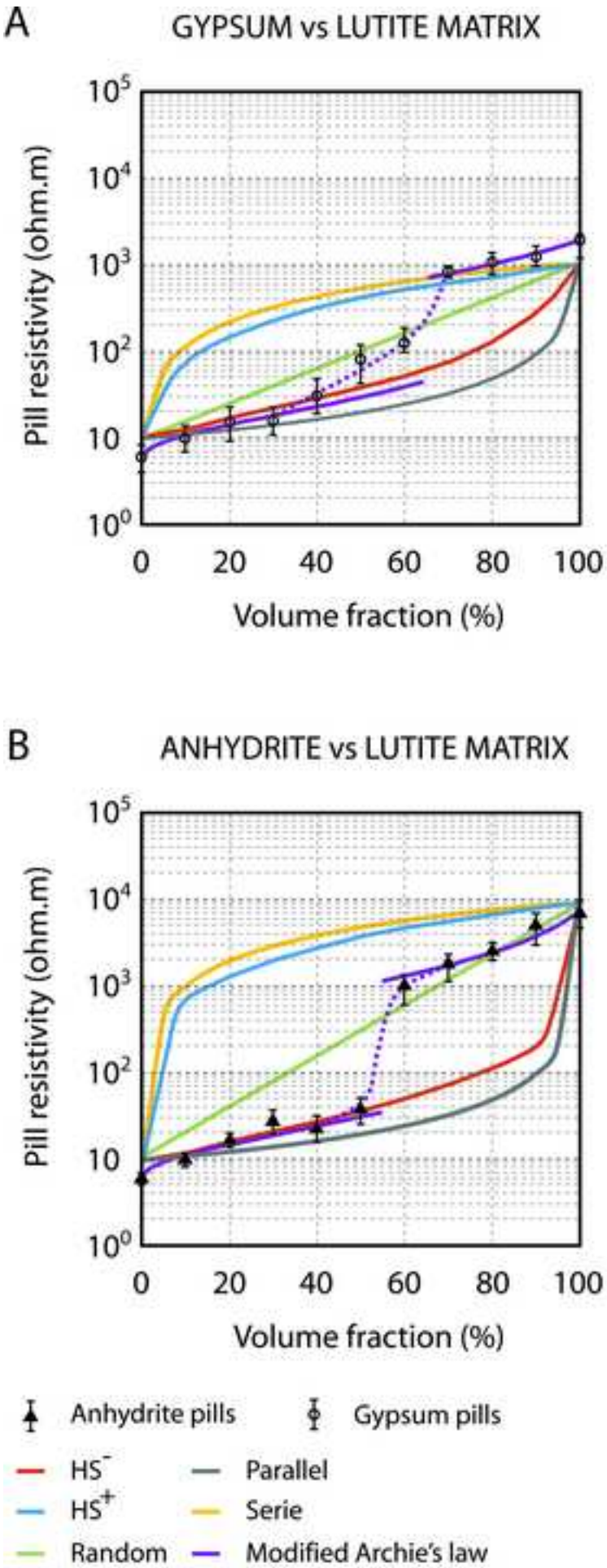

Figure 07

Click here to download high resolution image

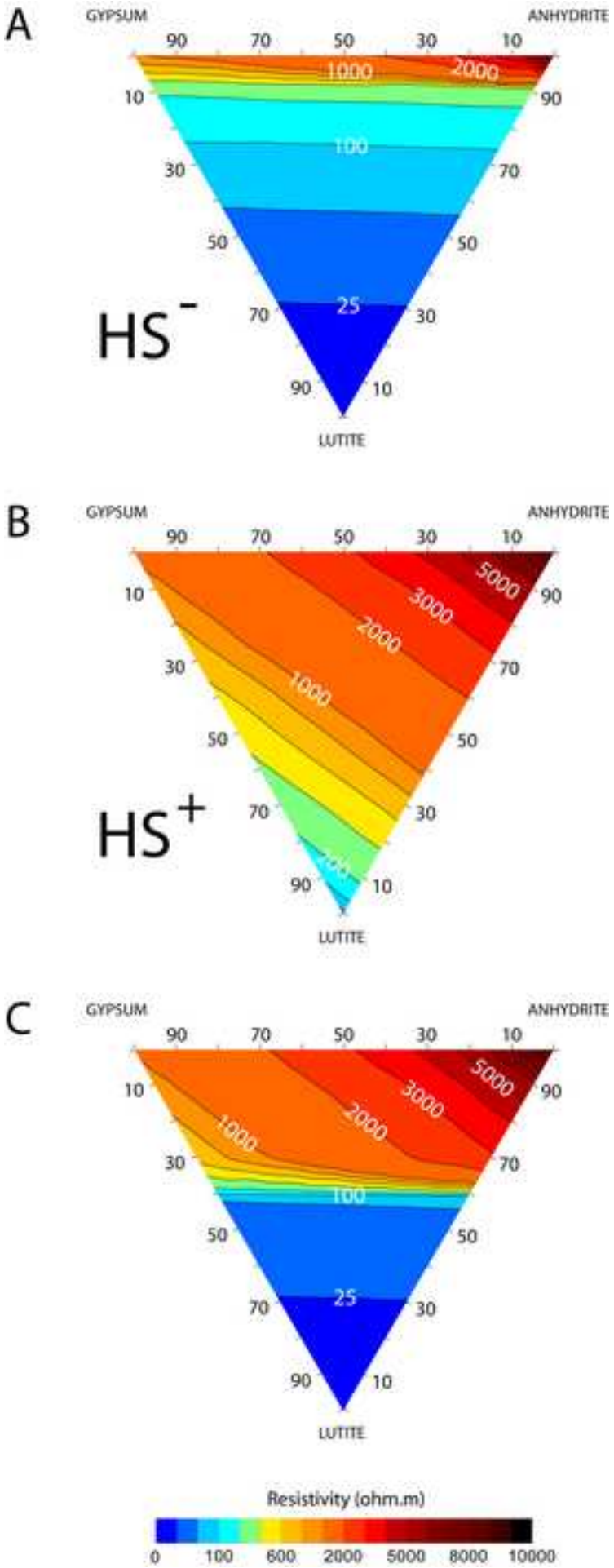

Figure 08

Click here to download high resolution image

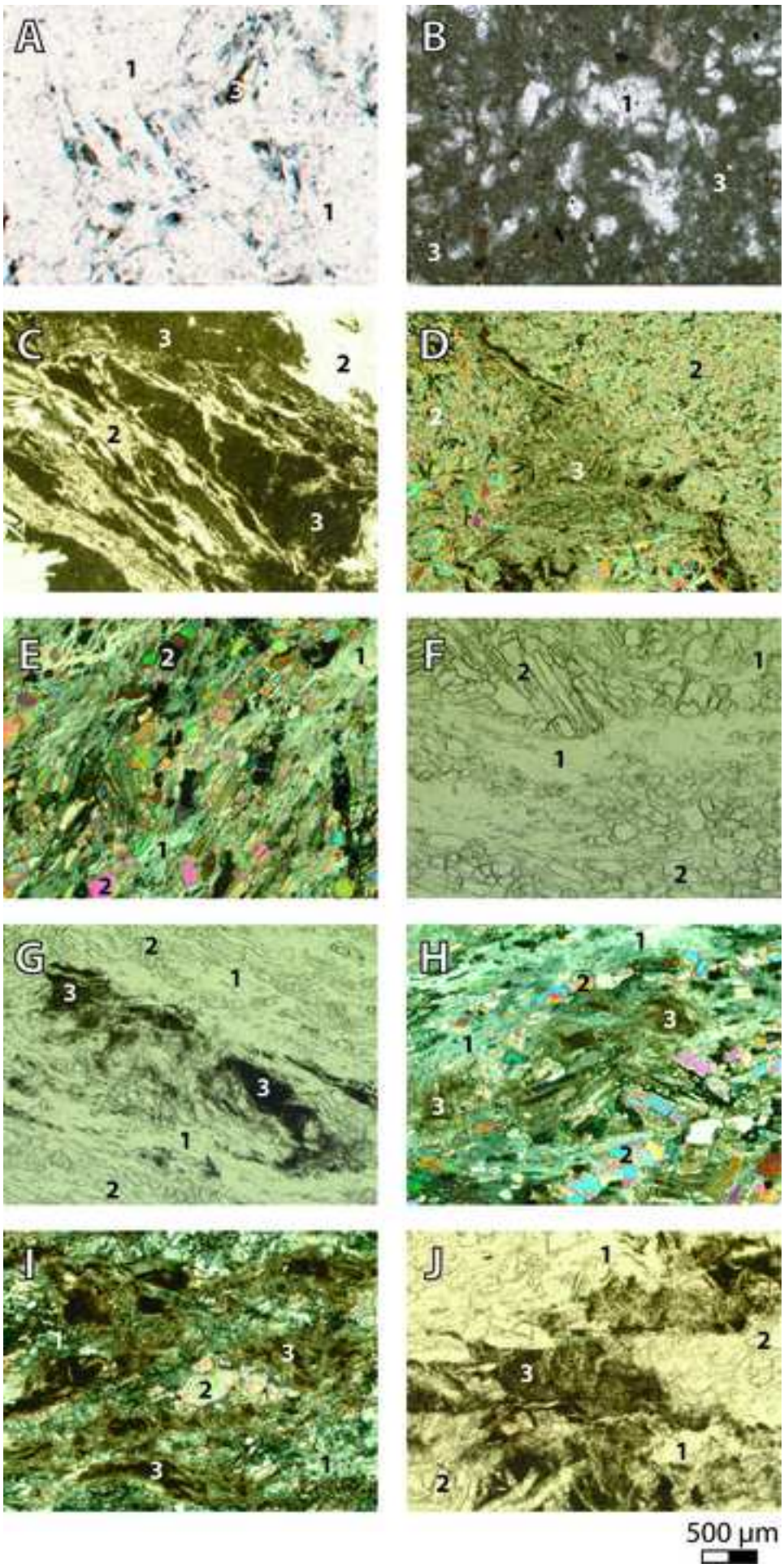

Figure 09

Click here to download high resolution image